Flavor-changing interactions with singlet quarks and their implications for the LHC

Katsuichi Higuchi
Department of Literature, Kobe Kaisei College, Kobe 657-0805, Japan

Katsuji Yamamoto
Department of Nuclear Engineering, Kyoto University, Kyoto 606-8501, Japan
(Received 9 November 2009; published 19 January 2010)

We investigate the flavor-changing interactions in an extension of the standard model with singlet quarks and singlet Higgs, which are induced by the mixing between the ordinary quarks and the singlet quarks (q-Q mixing). We consider the effects of the gauge and scalar interactions in the $\Delta F = 2$ mixings of K^0, B_d, B_s, and D^0 mesons to show the currently allowed range of the q-Q mixing. Then, we investigate the new physics around the electroweak scale to the TeV scale, which is accessible to the Large Hadron Collider. Especially, the scalar coupling mediated by the singlet Higgs may provide distinct signatures for the decays of the singlet quarks and Higgs particles, which should be compared with the conventionally expected ones via the gauge and standard Higgs couplings. Observations of the singlet quarks and Higgs particles will present us with important insights on the q-Q mixing and Higgs mixing.

DOI: 10.1103/PhysRevD.81.015009 PACS numbers: 12.60.−i, 12.15.−y, 14.65.Jk, 14.80.Ec

I. INTRODUCTION

As the standard model has been established in current experiments, the appearance of new physics now attracts growing interests especially in the light of the Large Hadron Collider (LHC). So far various extensions of the standard model with their own motivations have been investigated for new physics, including exotic fermions, extra Higgs fields, extended gauge interactions, supersymmetry, and so on. The new physics might already provide some significant effects in the low-energy particle phenomena such as flavor-changing processes. It is now expected seriously that the new physics will reveal itself in the LHC experiments.

Among many intriguing extensions of the standard model, we here investigate the new physics provided by isosinglet quarks, which are suggested in certain models such as E_6-type unification [1]. Specifically, there are two types of singlet quarks, U with electric charge $Q_{\rm em} = 2/3$ and D with $Q_{\rm em} = -1/3$, which may mix with the ordinary quarks. It is also reasonable to incorporate a singlet Higgs field S, which provides the singlet quark masses and the q-Q mixing between the ordinary quarks ($q = u$, d) and the singlet quarks ($Q = U$, D). In this sort of model various novel features arise through the q-Q mixing [2–27]. The unitarity of Cabibbo-Kobayashi-Maskawa (CKM) matrix within the ordinary quark sector is violated, and the flavor-changing neutral currents (FCNC's) appear at the tree level. These flavor-changing interactions are described appropriately in terms of the q-Q mixing parameters and quark masses [2,3,7,18,20]. Then, the actual CKM mixing is reproduced up to the small unitarity violation provided the FCNC's are suppressed sufficiently with the small q-Q mixing. In this respect the presence of singlet quarks may introduce an interesting extension of the notion of natural flavor conservation [28,29]. Furthermore, the new CP-violating phases in q-Q mixing may provide significant contributions especially in the B meson physics [2,3,8–10,12,14,15,19,22–27].

It is also expected in cosmology that the singlet quarks and singlet Higgs field may play important roles in the early universe. Specifically, in the first-order electroweak phase transition the CP-violating q-Q mixing via the coupling with the complex singlet Higgs S can be efficient to produce the chiral charge fluxes through the bubble wall for the baryogenesis [30,31]. Furthermore, the presence of singlet Higgs field is preferable for realizing the strong enough first-order electroweak phase transition.

As mentioned above, the singlet quarks and singlet Higgs bring various intriguing features in particle physics and cosmology. It is hence worth considering their phenomenological implications toward the discovery of them at the LHC [32–37]. In this study we investigate the flavor-changing interactions in the presence of singlet quarks and singlet Higgs. The effects of the gauge interactions have been investigated extensively in the literature [2–7,10–17,22–27]. Here, we rather note that the scalar interactions mediated by the singlet Higgs may provide significant effects in some cases [8,9,16,19,20], which has not been considered thoroughly so far in the models with singlet quarks.

The rest of this paper is organized as follows: In Sec. II, we describe a representative model with singlet quarks and one complex singlet Higgs field, and review the essential features on the quark mixings and flavor-changing interactions. In Sec. III, we consider the effects of the flavor-changing interactions in the $\Delta F = 2$ mixings of K^0, B_d, B_s, and D^0 mesons to show the currently allowed range of the q-Q mixing. In Sec. IV, we investigate the decays of the singlet quarks and Higgs particles, which may provide distinct signatures upon their productions at the LHC. Section V is devoted to summary. In the Appendix a detailed derivation is presented for the suitable relations among the gauge and scalar couplings.

II. QUARK MIXINGS AND FLAVOR-CHANGING INTERACTIONS

We first review the essential features on the quark mixings and flavor-changing interactions, including the singlet quarks and singlet Higgs, which are described appropriately in terms of the q-Q mixing parameters and quark masses (see Ref. [20] for the detailed description). We consider a representative electroweak model based on the gauge symmetry $\mathrm{SU}(3)_C \times \mathrm{SU}(2)_W \times \mathrm{U}(1)_Y$, where singlet quarks U and D together with one complex singlet Higgs field S are incorporated. The generic Yukawa couplings are given by

$$\begin{aligned}\mathcal{L}_{\mathrm{Y}} = &-u_0^c \lambda_u \Psi_{q_0} \Phi_H - U_0^c h_u \Psi_{q_0} \Phi_H - u_0^c (f_U S + f_U' S^\dagger) U_0 \\ &- U_0^c (\lambda_U S + \lambda_U' S^\dagger) U_0 - d_0^c \lambda_d V_0^\dagger \Psi_{q_0} \tilde{\Phi}_H \\ &- D_0^c h_d V_0^\dagger \Psi_{q_0} \tilde{\Phi}_H - d_0^c (f_D S + f_D' S^\dagger) D_0 \\ &- D_0^c (\lambda_D S + \lambda_D' S^\dagger) D_0 + \mathrm{H.c.}\end{aligned} \tag{1}$$

in terms of the two-component Weyl fields for the electroweak eigenstates with subscript "0." (The generation indices and Lorentz factors are omitted here for simplicity.) The isodoublets of left-handed ordinary quarks are represented by

$$\Psi_{q_0} = \begin{pmatrix} u_0 \\ V_0 d_0 \end{pmatrix} \tag{2}$$

with a certain 3×3 unitary matrix V_0. The Higgs doublet is also given by

$$\Phi_H = \begin{pmatrix} H^+ \\ H^0 \end{pmatrix} \tag{3}$$

with $\tilde{\Phi}_H \equiv i\tau_2 \Phi_H^*$. The Higgs fields develop vacuum expectation values (VEV's),

$$\langle H^0 \rangle = v/\sqrt{2}, \qquad \langle S \rangle = v_S/\sqrt{2}, \tag{4}$$

where $v = (\sqrt{2} G_F)^{-1/2} = 246$ GeV, and $v_S \sim$ 100 GeV–1 TeV is assumed. The possible complex phase δ_S of $\langle S \rangle$ is not presented explicitly for simplicity of notation, which may be effectively included in the Yukawa couplings and the Higgs potential terms at the tree level.

A. Quark masses and mixings

The quark mass matrix is produced as

$$\mathcal{M}_{\mathcal{Q}} = \begin{pmatrix} M_q & \Delta_{qQ} \\ \Delta'_{qQ} & M_Q \end{pmatrix}. \tag{5}$$

The submatrices are given by

$$M_q = \lambda_q v/\sqrt{2}, \qquad \Delta'_{qQ} = h_q v/\sqrt{2}, \tag{6}$$

$$\Delta_{qQ} = f_Q^+ v_S/\sqrt{2}, \qquad M_Q = \lambda_Q^+ v_S/\sqrt{2}, \tag{7}$$

where

$$f_Q^+ \equiv f_Q + f_Q', \qquad f_Q^- \equiv i(f_Q - f_Q'), \tag{8}$$

$$\lambda_Q^+ \equiv \lambda_Q + \lambda_Q', \qquad \lambda_Q^- \equiv i(\lambda_Q - \lambda_Q'). \tag{9}$$

Henceforth $\mathcal{Q} = (q, Q)$ collectively, and N_Q denotes the number of singlet quarks. The quark mass matrix $\mathcal{M}_{\mathcal{Q}}$ is diagonalized by unitary transformations $\mathcal{V}_{\mathcal{Q}_\mathrm{L}}$ and $\mathcal{V}_{\mathcal{Q}_\mathrm{R}}$ as

$$\mathcal{V}^\dagger_{\mathcal{Q}_\mathrm{R}} \mathcal{M}_{\mathcal{Q}} \mathcal{V}_{\mathcal{Q}_\mathrm{L}} = \bar{\mathcal{M}}_{\mathcal{Q}} = \begin{pmatrix} \bar{M}_q & \mathbf{0} \\ \mathbf{0} & \bar{M}_Q \end{pmatrix}, \tag{10}$$

where $\bar{M}_q = \mathrm{diag}(m_{q_1}, m_{q_2}, m_{q_3})$, $\bar{M}_Q = \mathrm{diag}(m_{Q_1}, \ldots)$, and $(q_1, q_2, q_3) = (u, c, t)$ or (d, s, b). The quark mass eigenstates q_i $(i = 1, 2, 3)$ and Q_a $(a = 1, 2, \ldots, N_Q)$ are given by

$$\begin{pmatrix} q \\ Q \end{pmatrix} = \mathcal{V}^\dagger_{\mathcal{Q}_\mathrm{L}} \begin{pmatrix} q_0 \\ Q_0 \end{pmatrix}, \qquad (q^c, Q^c) = (q_0^c, Q_0^c) \mathcal{V}_{\mathcal{Q}_\mathrm{R}} \tag{11}$$

with the $(3 + N_Q) \times (3 + N_Q)$ unitary matrices as

$$\mathcal{V}_{\mathcal{Q}_\chi} = \begin{pmatrix} V_{q_\chi} & \boldsymbol{\epsilon}_{q_\chi} \\ -\boldsymbol{\epsilon}'^\dagger_{q_\chi} & V_{Q_\chi} \end{pmatrix} \qquad (\chi = \mathrm{L, R}), \tag{12}$$

where $\boldsymbol{\epsilon}_{q_\chi}$ and $\boldsymbol{\epsilon}'_{q_\chi}$ represent the q-Q mixing.

The quark mass matrix $\mathcal{M}_{\mathcal{Q}}$ may be reduced to a specific form with either $\Delta'_{qQ} = \mathbf{0}$ or $\Delta_{qQ} = \mathbf{0}$ by a unitary transformation of the right-handed quarks. Then, the Yukawa coupling λ_q is diagonalized by unitary transformations of the ordinary quarks as

$$\lambda_q = \mathrm{diag}(\lambda_{q_1}, \lambda_{q_2}, \lambda_{q_3}), \tag{13}$$

while the condition $\Delta'_{qQ} = \mathbf{0}$ or $\Delta_{qQ} = \mathbf{0}$ is maintained. These transformations to specify the form of $\mathcal{M}_{\mathcal{Q}}$ do not mix the electroweak doublets with the singlets, respecting the $\mathrm{SU}(3)_C \times \mathrm{SU}(2)_W \times \mathrm{U}(1)_Y$. Hence, without loss of generality we may start with either of these bases,

b asis (a): $\Delta'_{qQ} = \mathbf{0}$, **basis (b)**: $\Delta_{qQ} = \mathbf{0}$.

The Yukawa couplings $h_q, f_Q, f'_Q, \lambda_Q, \lambda'_Q$ and the mixing matrix V_0 are redefined according to the transformations to specify the quark basis. In particular, $h_q = \mathbf{0}$ solely in the basis (a). On the other hand, in the basis (b) a specific relation $f'_Q = -f_Q$ $(f_Q^+ = \mathbf{0})$ holds apparently though no tuning is imposed among the couplings in the original basis.

The q-Q mixings are given specifically in the basis (a) as

$$(\boldsymbol{\epsilon}_{q_\mathrm{L}})_{ia} \sim (\boldsymbol{\epsilon}'_{q_\mathrm{L}})_{ia} \sim (m_{q_i}/m_Q)\boldsymbol{\epsilon}_i^f, \tag{14}$$

$$(\epsilon_{q_R})_{ia} \sim (\epsilon'_{q_R})_{ia} \sim \epsilon_i^f \quad (15)$$

in terms of the q-Q mixing parameters from the f_Q^+ coupling,

$$\epsilon_i^f = (v_S/m_Q)\overline{|(f_Q^+)_{ia}|}/\sqrt{2} = \overline{|(\Delta_{qQ})_{ia}|}/m_Q, \quad (16)$$

where $m_Q = \bar{m}_{Q_a} \sim (\overline{|(f_Q^+)_{ia}|} + \overline{|(\lambda_Q^+)_{ab}|})v_S$, and the bar denotes the mean value. The left-handed q-Q mixing is suppressed significantly by the q/Q mass ratios m_{q_i}/m_Q [2,3,7,18,20]. On the other hand, in the basis (b)

$$(\epsilon_{q_L})_{ia} \sim (\epsilon'_{q_L})_{ia} \sim \epsilon_i^h, \quad (17)$$

$$(\epsilon_{q_R})_{ia} \sim (\epsilon'_{q_R})_{ia} \sim (m_{q_i}/m_Q)\epsilon_i^h \quad (18)$$

in terms of the q-Q mixing parameters from the h_q coupling,

$$\epsilon_i^h = (v/m_Q)\overline{|(h_q)_{ai}|}/\sqrt{2} = \overline{|(\Delta'_{qQ})_{ai}|}/m_Q. \quad (19)$$

The left-handed q-Q mixing is no longer suppressed by the q/Q mass ratios.

We may move from the basis (a) with $\Delta'_{qQ} = \mathbf{0}$ to the basis (b) with $\Delta_{qQ} = \mathbf{0}$ by using a unitary transformation. Here, the left-handed q-Q mixings in the bases (a) and (b) are related as $\epsilon_i^h \sim (m_{q_i}/m_Q)\epsilon_i^f$ so that Eq. (14) is apparently reproduced from Eq. (17). Hence, the basis (a) may be regarded as a special case of the basis (b) [20]. If $\overline{|f_Q|} + \overline{|f'_Q|} \gtrsim \overline{|\lambda_Q|} + \overline{|\lambda'_Q|}$ providing $\epsilon_i^f \sim 1$ in the basis (a), then it is suitable to adopt the basis (b) alternatively. The seesaw basis with $M_q = \mathbf{0}$ is also possible for $N_Q = 3$ [38]. Since it is related to the bases (a) and (b) having a hybrid feature for the quark mixing [20], we do not consider explicitly the seesaw model. We adopt complementarily the bases (a) and (b), where the ordinary quark masses are reproduced as

$$m_{q_i} = c_i \lambda_{q_i} v/\sqrt{2} \quad (20)$$

with $c_i \sim 1$ depending on the small q-Q mixing [2,3,7,18,20]. In the general basis with $\Delta_{qQ} \neq \mathbf{0}$ and $\Delta'_{qQ} \neq \mathbf{0}$, e.g., the seesaw model, the ordinary quark mass hierarchy is not described clearly in terms of the Yukawa couplings λ_{q_i}.

B. Flavor-changing interactions

The CKM matrix V for the W-boson coupling with the ordinary quarks is given by

$$V = V_{u_L}^\dagger V_0 V_{d_L}, \quad (21)$$

where V_{u_L} and V_{d_L} are the 3×3 submatrices in Eq. (12). The unitarity violation of V is induced at the second order of q-Q mixing with $\epsilon_{q_L}\epsilon_{q_L}^\dagger$ and $\epsilon'_{q_L}\epsilon_{q_L}'^\dagger$, which should be suppressed enough phenomenologically [2–27]. Then, the realistic CKM matrix V is reproduced by taking suitably the original V_0.

The modification of the left-handed Z-boson coupling with the ordinary quarks is also given at the second order of q-Q mixing [2–27] as

$$\Delta Z_Q[q^\dagger q] = -\epsilon'_{q_L}\epsilon_{q_L}'^\dagger, \quad (22)$$

where the Z-boson coupling is presented by removing the isospin factor $I_3(q_0)$ with $I_3(u_0) = 1/2$ and $I_3(d_0) = -1/2$ for simplicity of notation. The right-handed coupling is, on the other hand, unchanged as $\Delta Z_{Q^c} = \mathbf{0}$ for $I_3(q_0^c) = I_3(Q_0^c) = 0$. Specifically, in the basis (a) we have

$$\Delta Z_Q[q^\dagger q]_{ij}(\mathrm{a}) \sim (m_{q_i}/m_Q)(m_{q_j}/m_Q)\epsilon_i^f \epsilon_j^f. \quad (23)$$

This correction as well as the CKM unitarity violation are suppressed substantially by the second order of q/Q mass ratios. Alternatively, in the basis (b) we have

$$\Delta Z_Q[q^\dagger q]_{ij}(\mathrm{b}) \sim \epsilon_i^h \epsilon_j^h, \quad (24)$$

which is no longer suppressed by the q/Q mass ratios. Then, significant constraints are placed phenomenologically on the q-Q mixings $\epsilon_i^h \ll 1$, which have been investigated extensively in the literature [10–17,22,23].

The neutral scalar couplings of the quarks $\mathcal{Q} = \mathcal{U}, \mathcal{D}$ are extracted from Eq. (1) as

$$\mathcal{L}_\phi(\mathcal{Q}) = -\sum_{\phi_r^0 = H, S_+, S_-} \mathcal{Q}^c \Lambda_{\mathcal{Q}}^{\phi_r^0} \mathcal{Q} \phi_r^0 + \mathrm{H.c.}, \quad (25)$$

where

$$\Lambda_{\mathcal{Q}}^H = \frac{1}{\sqrt{2}} \mathcal{V}_{\mathcal{Q}_R}^\dagger \begin{pmatrix} \lambda_q & \mathbf{0} \\ h_q & \mathbf{0} \end{pmatrix} \mathcal{V}_{\mathcal{Q}_L}, \quad (26)$$

$$\Lambda_{\mathcal{Q}}^{S_\pm} = \frac{1}{\sqrt{2}} \mathcal{V}_{\mathcal{Q}_R}^\dagger \begin{pmatrix} \mathbf{0} & f_Q^\pm \\ \mathbf{0} & \lambda_Q^\pm \end{pmatrix} \mathcal{V}_{\mathcal{Q}_L}. \quad (27)$$

The real neutral scalar fields, $\phi_1^0 = H \equiv \sqrt{2}\,\mathrm{Re}(H^0 - \langle H^0\rangle)$, $\phi_2^0 = S_+ \equiv \sqrt{2}\,\mathrm{Re}(S - \langle S\rangle)$, $\phi_3^0 = S_- \equiv \sqrt{2}\,\mathrm{Im}(S - \langle S\rangle)$, mix generally to form the mass eigenstates ϕ_r ($r = 1, 2, 3$) through an orthogonal transformation O_ϕ:

$$\begin{pmatrix} \phi_1 \\ \phi_2 \\ \phi_3 \end{pmatrix} = O_\phi \begin{pmatrix} H \\ S_+ \\ S_- \end{pmatrix}. \quad (28)$$

The Nambu-Goldstone mode $G \equiv \sqrt{2}\,\mathrm{Im}(H^0 - \langle H^0\rangle)$ is absorbed by the Z boson.

The submatrices $\Lambda_{\mathcal{Q}}^{\phi_r^0}[q^c q]$ of these neutral scalar couplings for the ordinary quarks are given by

$$\Lambda_{\mathcal{Q}}^H[q^c q] = V_{q_R}^\dagger \lambda_q V_{q_L} - \epsilon'_{q_R} h_q V_{q_L}, \quad (29)$$

$$\Lambda_{\mathcal{Q}}^{S_\pm}[q^c q] = -V_{q_R}^\dagger f_Q^\pm \epsilon_{q_L}'^\dagger + \epsilon'_{q_R} \lambda_Q^\pm \epsilon_{q_L}'^\dagger. \quad (30)$$

Here, some close relations hold for the gauge and scalar couplings (see the Appendix for derivation). The coupling of the standard Higgs H is given actually as

$$\Lambda_Q^H[q^c q]_{ij} = (m_{q_i}/v)(\delta_{ij} + \Delta Z_Q[q^\dagger q]_{ij}) \tag{31}$$

with the q-Q mixing induced Z-boson coupling $\Delta Z_Q[q^\dagger q]$ in Eq. (22). Similarly, the coupling of the singlet Higgs S_+ is calculated as

$$\Lambda_Q^{S_+}[q^c q]_{ij} = -(m_{q_i}/v_S)\Delta Z_Q[q^\dagger q]_{ij}. \tag{32}$$

Hence, the q-Q mixing effects for the scalar couplings $\Lambda_Q^H[q^c q]$ and $\Lambda_Q^{S_+}[q^c q]$ are always subleading compared with those for the Z-boson coupling $\Delta Z_Q[q^\dagger q]$, which is due to the suppression by m_{q_i}/v from the chirality flip. It is rather remarkable that the coupling of the singlet Higgs S_- may be dominant without a close relation to the Z-boson coupling. In the basis (a) we have

$$\Lambda_Q^{S_-}[q^c q]_{ij}(\mathrm{a}) \sim (m_{q_j}/v_S)\epsilon_i^f \epsilon_j^f, \tag{33}$$

where $(\epsilon'^\dagger_{q_L})_{aj} \sim (m_{q_j}/m_Q)\epsilon_j^f$, $(\epsilon'_{q_R})_{ia} \sim \epsilon_i^f$, $(\lambda_Q^-)_{ab} \sim (m_Q/v_S)$ and $(f_Q^-)_{ia} \sim (m_Q/v_S)\epsilon_i^f$ are applied in Eq. (30). In contrast to the Z-boson coupling $\Delta Z_Q[q^\dagger q]$ in Eq. (23), the scalar coupling $\Lambda_Q^{S_-}[q^c q]$ in Eq. (33) is suppressed only by the first order of ordinary quark mass. In the basis (b), by applying $(\epsilon'^\dagger_{q_L})_{aj} \sim \epsilon_j^h$ and $(f_Q^-)_{ia} \sim (m_Q/v_S)\epsilon_i^f$ in Eq. (30), we estimate

$$\Lambda_Q^{S_-}[q^c q]_{ij}(\mathrm{b}) \sim (m_Q/v_S)\epsilon_i^f \epsilon_j^h, \tag{34}$$

up to the subleading contribution of the second term $\sim (m_{q_i}/v_S)\epsilon_i^h \epsilon_j^h$ in Eq. (30). Here, similar to Eq. (16), the q-Q mixing parameters are introduced for convenience as $\epsilon_i^f = (v_S/m_Q)|2(f_Q)_{ia}|/\sqrt{2}$ even though $f_Q^+ = \mathbf{0}$ ($f_Q^- = 2if_Q$ with $f_Q = -f'_Q$) for $\Delta_{qQ} = \mathbf{0}$ in the basis (b). It should also be noted, as discussed previously, that by considering the relation for the left-handed q-Q mixing,

$$\epsilon_i^h \sim (m_{q_i}/m_Q)\epsilon_i^f, \tag{35}$$

Eqs. (24) and (34) in the basis (b) reproduce Eqs. (23) and (33) in the basis (a), respectively.

We mention for completeness that in the case of one real S (or one supersymmetric S) with the f_Q and λ_Q couplings ($f'_Q \equiv \mathbf{0}$ and $\lambda'_Q \equiv \mathbf{0}$), the scalar coupling $\Lambda_Q^S[q^c q]$ is given by Eq. (32) for $\Lambda_Q^{S_+}[q^c q]$ related to the Z-boson coupling $\Delta Z_Q[q^\dagger q]$. On the other hand, if the bare mass term M_Q is adopted instead of the λ_Q coupling while the f_Q coupling provides the q-Q mixing, the scalar coupling $\Lambda_Q^S[q^c q]$ is rather given by Eqs. (33) and (34) for $\Lambda_Q^{S_-}[q^c q]$ even in the case of one real S.

III. SINGLET QUARK EFFECTS IN $\Delta F = 2$ MIXINGS OF NEUTRAL MESONS

We perform a detailed analysis on the q-Q mixing effects in the $\Delta F = 2$ mixings of K^0, B_d, B_s and D^0 mesons, by considering the general bounds for new physics which are presented in Ref. [39]. The Z-mediated FCNC's in $\Delta Z_Q[q^\dagger q]$ have been investigated extensively in the literature [2–7,10–17,22–27]. By placing experimental constraints on the left-handed q-Q mixings $(\epsilon_{q_L})_{ia} \sim (\epsilon'_{q_L})_{ia} \sim \epsilon_i^h$ in the basis (b), these analyses have discussed the possibility of new physics provided by the singlet quarks, in particular, for the B meson physics. Here, we rather note that in some cases the scalar FCNC's in $\Lambda_Q^{S_-}[q^c q]$ may dominate over the Z-mediated FCNC's in $\Delta Z_Q[q^\dagger q]$, providing distinct signals for new physics [8,9,16,19,20]. This intriguing possibility has not been paid so much attention so far in the models with singlet quarks.

The effective Hamiltonian contributing to the $\Delta F = 2$ mixing of the neutral meson M (K^0, B_d, B_s, D^0) is given generally [39] as

$$\mathcal{H}_{\mathrm{eff}}^{\Delta F=2} = \sum_{k=1}^{5} C_M^k \mathcal{O}_k^{q_i q_j} + \sum_{k=1}^{3} \tilde{C}_M^k \tilde{\mathcal{O}}_k^{q_i q_j}, \tag{36}$$

where

$$q_i q_j = sd(K^0), bd(B_d), bs(B_s), cu(D^0). \tag{37}$$

The four-quark operators are

$$\mathcal{O}_1^{q_i q_j} = \bar{q}_{j\mathrm{L}}^\alpha \gamma_\mu q_{i\mathrm{L}}^\alpha \bar{q}_{j\mathrm{L}}^\beta \gamma^\mu q_{i\mathrm{L}}^\beta, \qquad \mathcal{O}_2^{q_i q_j} = \bar{q}_{j\mathrm{R}}^\alpha q_{i\mathrm{L}}^\alpha \bar{q}_{j\mathrm{R}}^\beta q_{i\mathrm{L}}^\beta,$$
$$\mathcal{O}_3^{q_i q_j} = \bar{q}_{j\mathrm{R}}^\alpha q_{i\mathrm{L}}^\beta \bar{q}_{j\mathrm{R}}^\beta q_{i\mathrm{L}}^\alpha, \qquad \mathcal{O}_4^{q_i q_j} = \bar{q}_{j\mathrm{R}}^\alpha q_{i\mathrm{L}}^\alpha \bar{q}_{j\mathrm{L}}^\beta q_{i\mathrm{R}}^\beta,$$
$$\mathcal{O}_5^{q_i q_j} = \bar{q}_{j\mathrm{R}}^\alpha q_{i\mathrm{L}}^\beta \bar{q}_{j\mathrm{L}}^\beta q_{i\mathrm{R}}^\alpha,$$

and α and β denote the colors. The operators $\tilde{\mathcal{O}}_{1,2,3}^{q_i q_j}$ are obtained from the operators $\mathcal{O}_{1,2,3}^{q_i q_j}$ by the exchange L $\leftrightarrow$ R. The coefficients in the effective Hamiltonian at the scale $\mu = m_Q$ of singlet quarks are calculated as

$$C_M^1(m_Q) = (g/2\cos\theta_W)^2(\Delta Z_Q[q^\dagger q]_{ji})^2/m_Z^2, \tag{38}$$

$$C_M^2(m_Q) = (\Lambda_Q^{S_-}[q^c q]_{ji})^2/m_{S_-}^2, \tag{39}$$

$$\tilde{C}_M^2(m_Q) = (\Lambda_Q^{S_-}[q^c q]_{ij}^*)^2/m_{S_-}^2, \tag{40}$$

$$C_M^4(m_Q) = (\Lambda_Q^{S_-}[q^c q]_{ji})(\Lambda_Q^{S_-}[q^c q]_{ij}^*)/m_{S_-}^2, \tag{41}$$

and the others are zero. Here, the Z-boson coupling $\Delta Z_Q[q^\dagger q]$ and the dominant scalar coupling $\Lambda_Q^{S_-}[q^c q]$ are considered, and the scalar mixing in O_ϕ is neglected for simplicity. By requiring that these coefficients in Eqs. (38)–(41) are all within the bounds presented specifically in Table 4 of Ref. [39], we find the allowed range of the q-Q mixing depending on the masses $m_Q, m_{S_-} \sim v_S$ of the singlet quarks Q and singlet Higgs S_-.

The constraints on the q-Q mixing are given roughly below, where $m_D = m_U = v_S = 500$ GeV and $m_{S_-} = 0.6 v_S = 300$ GeV are taken typically to estimate the FCNC's with Eqs. (23), (24), (33), and (34) in terms of the q-Q mixing parameters ϵ_i^f and ϵ_i^h. In the basis (a) significant constraints on the d-D mixing are placed by the scalar coupling $\Lambda_{\mathcal{D}}^{S_-}[d^c d]$ for C_M^2, $\tilde{C}_M^2$ and C_M^4 ($M = K^0, B_d, B_s$) as

$$\Lambda_{\mathcal{D}}^{S_-}(\mathrm{a}): \quad \begin{array}{ll} (\epsilon_1^f \epsilon_2^f)^{1/2} \lesssim 0.1/\delta_{12}^{1/4} & (\mathrm{Im} K) \\ (\epsilon_1^f \epsilon_2^f)^{1/2} \lesssim 0.4 & (\mathrm{Re} K) \\ (\epsilon_1^f \epsilon_3^f)^{1/2} \lesssim 0.2 & (|B_d|) \\ (\epsilon_2^f \epsilon_3^f)^{1/2} \lesssim 0.5 & (|B_s|). \end{array} \tag{42}$$

Here, the effective CP-violating phases in the FCNC's contributing to the K^0-$\bar{K}^0$ mixing are denoted collectively by δ_{12}. No significant constraints are, on the other hand, placed by the Z-boson coupling $\Delta Z_{\mathcal{D}}[d^\dagger d]$ which is substantially suppressed by the second order of d/D mass ratios in Eq. (23). Alternatively, in the basis (b) constraints on the d-D mixing are given as

$$\Lambda_{\mathcal{D}}^{S_-}(\mathrm{b}): \quad \begin{array}{ll} (\epsilon_1^f \epsilon_2^h)^{1/2}, (\epsilon_2^f \epsilon_1^h)^{1/2} \lesssim 1 \times 10^{-3}/\delta_{12}^{1/4} & (\mathrm{Im} K) \\ (\epsilon_1^f \epsilon_2^h)^{1/2}, (\epsilon_2^f \epsilon_1^h)^{1/2} \lesssim 4 \times 10^{-3} & (\mathrm{Re} K) \\ (\epsilon_1^f \epsilon_3^h)^{1/2}, (\epsilon_3^f \epsilon_1^h)^{1/2} \lesssim 0.01 & (|B_d|) \\ (\epsilon_2^f \epsilon_3^h)^{1/2}, (\epsilon_3^f \epsilon_2^h)^{1/2} \lesssim 0.03 & (|B_s|), \end{array} \tag{43}$$

$$\Delta Z_{\mathcal{D}}(\mathrm{b}): \quad \begin{array}{ll} (\epsilon_1^h \epsilon_2^h)^{1/2} \lesssim 4 \times 10^{-3}/\delta_{12}^{1/4} & (\mathrm{Im} K) \\ (\epsilon_1^h \epsilon_2^h)^{1/2} \lesssim 0.02 & (\mathrm{Re} K) \\ (\epsilon_1^h \epsilon_3^h)^{1/2} \lesssim 0.03 & (|B_d|) \\ (\epsilon_2^h \epsilon_3^h)^{1/2} \lesssim 0.09 & (|B_s|). \end{array} \tag{44}$$

Here, the constraints for the basis (a) in Eq. (42) are reproduced roughly from those for the basis (b) in Eq. (43) under the relation in Eq. (35). Constraints on the u-U mixing are estimated in the bases (a) and (b) as

$$\Lambda_{\mathcal{U}}^{S_-}(\mathrm{a}): (\epsilon_1^f \epsilon_2^f)^{1/2} \lesssim 0.2 \qquad (|D^0|), \tag{45}$$

$$\Lambda_{\mathcal{U}}^{S_-}(\mathrm{b}): (\epsilon_1^f \epsilon_2^h)^{1/2}, (\epsilon_2^f \epsilon_1^h)^{1/2} \lesssim 8 \times 10^{-3} \qquad (|D^0|), \tag{46}$$

$$\Delta Z_{\mathcal{U}}(\mathrm{b}): (\epsilon_1^h \epsilon_2^h)^{1/2} \lesssim 0.01 \qquad (|D^0|). \tag{47}$$

Here, we comment on the contributions of the one-loop diagrams involving the singlet quarks and gauge bosons, which are enhanced by the factor $(m_Q/m_W)^2 g^2/(4\pi)^2$ compared with the tree-diagram contributions considered so far. They may dominate over the tree-diagram contributions for $m_Q > 1$ TeV, though we are mainly interested in the singlet quarks below 1 TeV in this analysis. The allowed range of the q-Q mixing will hence be reduced slightly for $m_Q \sim 1$ TeV. However, for a larger $m_Q \sim 10$ TeV, the loop contributions decrease as $(\epsilon_i^h \epsilon_j^h)^2 \times (m_Q/m_W)^2 \propto 1/m_Q^2$ with $\epsilon_i^h \propto 1/m_Q$ in Eq. (19). In such a case of $m_Q \sim 10$ TeV, the gauge-mediated q-Q mixing effects to the $\Delta F = 2$ meson mixings are anyway below the current experimental bounds since the q-Q mixing becomes significantly small as $\epsilon_i^h < 0.02$ for $\overline{|(h_q)_{ai}|} < 1$ in Eq. (19).

In supplement to the above constraints on the q-Q mixing parameters from the FCNC's, it is also relevant to consider the constraints from the flavor-diagonal Z-boson couplings [7,11,14]. The observed branching ratios of the decays $Z \to q_i \bar{q}_i$ imply that the deviations of the flavor-diagonal Z-boson couplings from the standard model values should be small enough. Specifically, in the basis (b) with Eq. (24) constraints on the q-Q mixing may be placed roughly as

$$\Delta Z_Q(\mathrm{b}): \epsilon_i^h \lesssim 0.03 \leftarrow |\Delta Z_Q[q^\dagger q]_{ii}| \lesssim 10^{-3}. \tag{48}$$

On the other hand, in the basis (a) $\Delta Z_Q[q^\dagger q]_{ii}$ of Eq. (23) is safely suppressed by $(m_{q_i}/m_Q)^2$ except for $q_i = t$.

To be more quantitative, we present the results of detailed numerical calculations for the d-D mixing effects in the down-type quark sector with one singlet D quark ($N_D = 1$ and $N_U = 0$) as a typical case. We take various values for the model parameters in a reasonable range as

$$\begin{aligned} v = 246\ \mathrm{GeV}, \qquad v_S = 500\ \mathrm{GeV}, \\ \lambda_{d_i} = \lambda_{d_i}^{(0)} = \sqrt{2} m_{d_i}/v \qquad (\mathrm{preliminary}), \\ |\lambda_D|, |\lambda'_D| \in [0.3, 1.0] \sim m_D/v_S, \\ (v/v_S)|(h_d)_i|/|\lambda_D^+| \in [0, 0.05] \sim \epsilon_i^h, \\ |(f_D)_i|/|\lambda_D^+|, |(f'_D)_i|/|\lambda_D^+| \in [0, 2.0] \sim \epsilon_i^f, \\ \arg[h_d, f_D, f'_D, \lambda_D, \lambda'_D] \in [-0.3\pi, 0.3\pi]. \end{aligned}$$

Here, the VEV v_S of the singlet Higgs S is fixed to a typical value for definiteness. The complex phases of the Yukawa couplings $h_d, f_D, f'_D, \lambda_D, \lambda'_D$ contribute to the CP violation in the FCNC's such as δ_{12} for ϵ_K of the K^0-$\bar{K}^0$ mixing. The total quark mass matrix $\mathcal{M}_{\mathcal{D}}$ (4×4 for $N_D = 1$) in Eq. (5) is given for a set of values of the model parameters. This preliminary $\mathcal{M}_{\mathcal{D}}$ with $\lambda_{d_i} = \lambda_{d_i}^{(0)}$ is diagonalized to evaluate the eigenvalues $m_{d_i}^{(0)}$ for the ordinary quark masses. Then, by considering the ratios $m_{d_i}^{(0)}/m_{d_i} \sim 1$ we adjust λ_{d_i} to obtain the actual quark masses m_{d_i}:

$$\lambda_{d_i} \to m_d = 5\ \mathrm{MeV}, \quad m_s = 110\ \mathrm{MeV}, \quad m_b = 4.2\ \mathrm{GeV}.$$

The singlet quark mass m_D is obtained for the above range of the model parameters as

$$m_D \sim 100\ \mathrm{GeV}\text{–}1\ \mathrm{TeV} \qquad (v_S = 500\ \mathrm{GeV}).$$

At the same time, the unitary transformations $\mathcal{V}_{\mathcal{D}_\mathrm{L}}$ and

$\mathcal{V}_{\mathcal{D}_\mathrm{R}}$ to specify the quark mass eigenstates are calculated. The actual CKM matrix V is reproduced by adjusting the original unitary matrix V_0 as $V_0 = VV_{d_\mathrm{L}}^{-1} \simeq VV_{d_\mathrm{L}}^\dagger$ ($V_{u_\mathrm{L}} = \mathbf{1}$ for $N_U = 0$):

$$V_0 \to V(\mathrm{CKM}).$$

As long as the q-Q mixing is small enough to satisfy the constraints from the $\Delta F = 2$ meson mixings, the unitarity violation of the CKM matrix is safely suppressed.

By using these results on the quark masses and q-Q mixings, we evaluate the couplings of the quarks with the gauge bosons and Higgs particles. Then, the contributions of the d-D mixing induced FCNC's to the effective Hamiltonian $\mathcal{H}_{\mathrm{eff}}^{\Delta F=2}$ for the K^0, B_d and B_s mixings are evaluated with Eqs. (38)–(41). They are compared with the experimental bounds presented in Table 4 of Ref. [39] to find the allowed range of the d-D mixing parameters ϵ_i^f and ϵ_i^h. In this analysis, the masses of the Higgs particles are taken typically as

$$m_H = 120\ \mathrm{GeV}, \qquad m_{S_+} = m_{S_-} = 300\ \mathrm{GeV}. \tag{49}$$

Note here that the contributions of the S_- coupling in Eqs. (39)–(41) are proportional to $1/m_{S_-}^2$. Hence, as m_{S_-} is larger, the allowed range of the q-Q mixing parameters is extended further.

We have made the above calculations for many samples of the model parameter values. We show some characteristic results in the following. The portions of the $d - D$ mixing effects in the $\Delta F = 2$ meson mixings for the experimental bounds $|C_M^k|_{\max}$ [39] are denoted by

$$r_k(M) \equiv |C_M^k|/|C_M^k|_{\max}. \tag{50}$$

In Fig. 1 scatter plots of $r_2(B_d)$(○) and $r_2(B_s)$ (▲) versus $(\epsilon_1^f\epsilon_3^f)^{1/2}$ are shown for the B_d-$\bar{B}_d$ and B_s-$\bar{B}_s$ mixings, respectively, which are provided by the singlet S_- coupling $\Lambda_{\mathcal{D}}^{S_-}[d^c d]$ in the basis (a). Similar plots of $r_2(B_s)$ (▲) and $r_2(B_d)$ (○) versus $(\epsilon_2^f\epsilon_3^f)^{1/2}$ are shown in Fig. 2. The bounds for the K^0-$\bar{K}^0$ mixing have been checked to be satisfied in these plots. The results in Figs. 1 and 2 are in accordance with the rough estimates to obtain the bounds in Eq. (42). The dominant effects of the S_- coupling $\Lambda_{\mathcal{D}}^{S_-}[d^c d]$ of Eq. (33) are estimated in Eq. (39) as $|C_{B_d}^2| \sim (m_b/v_S)^2(\epsilon_1^f\epsilon_3^f)^2/m_{S_-}^2$ and $|C_{B_s}^2| \sim (m_b/v_S)^2(\epsilon_2^f\epsilon_3^f)^2/m_{S_-}^2$. In the log-log plot of Fig. 1, $r_2(B_d)$ (○)shows roughly the expected linear correlation with $(\epsilon_1^f\epsilon_3^f)^{1/2}$, while $r_2(B_s)$ (▲) are distributed independently of $(\epsilon_1^f\epsilon_3^f)^{1/2}$. We see the similar feature in Fig. 2 for $r_2(B_s)$ (▲) and $r_2(B_d)$ (○) versus $(\epsilon_2^f\epsilon_3^f)^{1/2}$. Precisely, in the basis (a) the d-D mixing parameters ϵ_i^f are defined with the f_D^+ coupling, while the singlet S_- coupling $\Lambda_{\mathcal{D}}^{S_-}$ is given by the f_D^- coupling ($|f_D^+| \sim |f_D^-|$ generally). This fact provides the appreciable spreads in the plots of $r_2(B_d)$ versus $(\epsilon_1^f\epsilon_3^f)^{1/2}$ and $r_2(B_s)$ versus $(\epsilon_2^f\epsilon_3^f)^{1/2}$. We find in these plots that the d-D mixing parameters $(\epsilon_1^f\epsilon_3^f)^{1/2}$ and $(\epsilon_2^f\epsilon_3^f)^{1/2}$ are really constrained for $r_2(B_d) \leq 1$ and $r_2(B_s) \leq 1$, respectively, as shown in Eq. (42). We note particularly that both the bounds for the B_d-$\bar{B}_d$ and B_s-$\bar{B}_s$ mixings may be saturated simultaneously with $\epsilon_3^f \sim 1$ and $(\epsilon_1^f\epsilon_2^f)^{1/2} \sim 0.1$ without conflicting with the bonds for the K^0-$\bar{K}^0$ mixing. Generally, in the basis (a) the right-handed d-D mixing is rather tolerable with $\epsilon_i^f \sim 0.1$–1. This is because the right-handed components of the ordinary and singlet quarks are indistinguishable with respect to the gauge interactions.

In Fig. 3 scatter plots of $r_1(B_d)$ (●) and $r_2(B_d)$ (○) versus $(\epsilon_1^h\epsilon_3^h)^{1/2}$ are shown for the B_d-$\bar{B}_d$ mixing, which

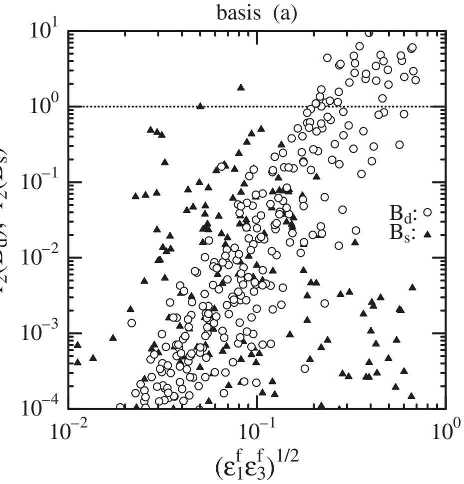

FIG. 1. Scatter plots of $r_2(B_d) \equiv |C_{B_d}^2|/|C_{B_d}^2|_{\max}$ (○) and $r_2(B_s) \equiv |C_{B_s}^2|/|C_{B_s}^2|_{\max}$ (▲) versus $(\epsilon_1^f\epsilon_3^f)^{1/2}$ for the B_d-$\bar{B}_d$ and B_s-$\bar{B}_s$ mixings, respectively, which are provided by the S_- coupling $\Lambda_{\mathcal{D}}^{S_-}[d^c d]$ in the basis (a).

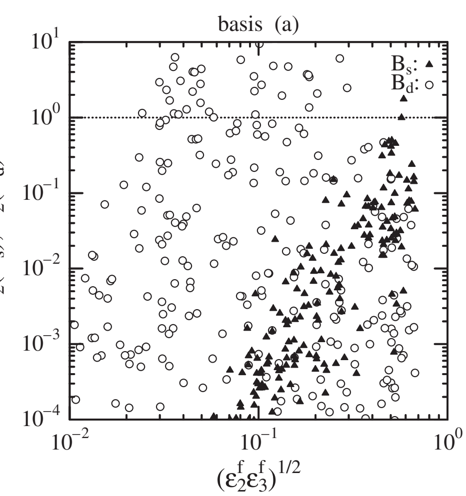

FIG. 2. Scatter plots of $r_2(B_s) \equiv |C_{B_s}^2|/|C_{B_s}^2|_{\max}$ (▲) and $r_2(B_d) \equiv |C_{B_d}^2|/|C_{B_d}^2|_{\max}$ (○) versus $(\epsilon_2^f\epsilon_3^f)^{1/2}$, similarly to Fig. 1.

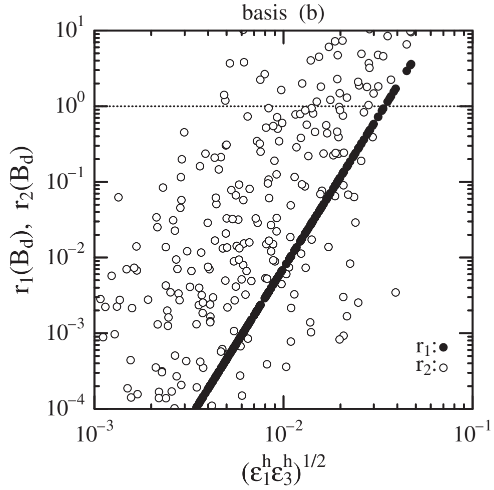

FIG. 3. Scatter plots of $r_1(B_d) \equiv |C^1_{B_d}|/|C^1_{B_d}|_{\max}$ (●) and $r_2(B_d) \equiv |C^2_{B_d}|/|C^2_{B_d}|_{\max}$ (○) versus $(\epsilon_1^h\epsilon_3^h)^{1/2}$ for the B_d-$\bar{B}_d$ mixing, which are provided by the Z coupling $\Delta Z_{\mathcal{D}}[d^\dagger d]$ and the S_- coupling $\Lambda^{S_-}_{\mathcal{D}}[d^c d]$, respectively, in the basis (b).

are provided by the Z-boson coupling $\Delta Z_{\mathcal{D}}[d^\dagger d]$ and the singlet S_- coupling $\Lambda^{S_-}_{\mathcal{D}}[d^c d]$, respectively, in the basis (b). Similar plots of $r_1(B_s)$ (△) and $r_2(B_s)$ (▲) versus $(\epsilon_2^h\epsilon_3^h)^{1/2}$ are shown in Fig. 4 for the B_s-$\bar{B}_s$ mixing. The bounds for the K^0-$\bar{K}^0$ mixing have been checked to be satisfied in these plots. The flavor-diagonal Z-boson couplings have also been checked to satisfy $|\Delta Z_{\mathcal{Q}}[q^\dagger q]_{ii}| < 3 \times 10^{-3}$, as considered in Eq. (48). The effects of the Z-boson coupling $\Delta Z_{\mathcal{Q}}[q^\dagger q]$ of Eq. (24) are estimated in Eq. (38) for the basis (b) as $|C^1_{B_d}| \sim (\epsilon_1^h\epsilon_3^h)^2\sqrt{2}G_F$ and $|C^1_{B_s}| \sim (\epsilon_2^h\epsilon_3^h)^2 \times \sqrt{2}G_F$. In the log-log plot of Fig. 3, $r_1(B_d)$ (●) shows clearly the linear correlation with $(\epsilon_1^h\epsilon_3^h)^{1/2}$ [here more precisely $(\epsilon_{q_L})_i \simeq (\epsilon'_{q_L})_i \simeq \epsilon_i^h$ for the left-handed q-Q mixing]. This is also the case in Fig. 4 for $r_1(B_s)$ (△) versus $(\epsilon_2^h\epsilon_3^h)^{1/2}$. The d-D mixing with $\epsilon_1^h \sim 0.03$ and $\epsilon_3^h \sim 0.03$ may saturate the bound for the B_d-$\bar{B}_d$ mixing via the Z-boson coupling, $r_1(B_d) \equiv |C^1_{B_d}|/|C^1_{B_d}|_{\max} \approx 1$, as seen in Fig. 3, which also provides significant effects ~0.1% on the flavor-diagonal Z-boson couplings in Eq. (48). On the other hand, as long as $\epsilon_i^h \lesssim 0.03$, the d-D mixing effect $C^1_{B_s}$ via the Z-boson coupling is fairly below the bound for the B_s-$\bar{B}_s$ mixing, $r_1(B_s) \equiv |C^1_{B_s}|/|C^1_{B_s}|_{\max} < 0.1$, as seen in Fig. 4. It should be noted here that as seen in Figs. 3 and 4, the contributions $C^2_{B_d}$ (○) and $C^2_{B_s}$ (▲) via the singlet S_- coupling $\Lambda^{S_-}_{\mathcal{D}}[d^c d]$ of Eq. (34) may dominate over the Z-boson coupling effects in the parameter region of $\epsilon_i^f > \epsilon_i^h$, where the bounds in Eq. (43) are applicable. In particular, the case of $\epsilon_i^f \gg \epsilon_i^h$ is connected gradually to a suitable parameter region in the basis (a).

In short, remarkable effects may be provided particularly for the B mesons through the significant mixing between the b quark and the singlet D quark with $\epsilon_3^f \sim 1$ or $\epsilon_3^h \sim 0.03$, as seen in the above. They are fairly expected to serve as new physics for the flavor-changing processes and CP-violation in the B meson physics [2,3,8–10,12,14,15,19,22–27,40]. Specifically, it is well known that there is tension between the experimental constraints and the standard model contribution to the $b \to s\gamma$ process, and hence this process should not be used as a constraint at present. The recent constraint by HFAG [41] is given as the average of the data of *BABAR*, Belle, and CLEO, $\mathrm{Br}(b \to s\gamma) = (352 \pm 23 \pm 9) \times 10^{-6}$, while the recent predictions of the standard model contribution are given as $\mathrm{Br}(b \to s\gamma) = (315 \pm 23) \times 10^{-6}$ [42] and $\mathrm{Br}(b \to s\gamma) = (298 \pm 26) \times 10^{-6}$ [43]. Even though this discrepancy is small, it may be confirmed by future experiments. The FCNC's via the d-D mixing can provide a solution of the discrepancy. This topic is, however, beyond the scope of the present work, and will be studied elsewhere.

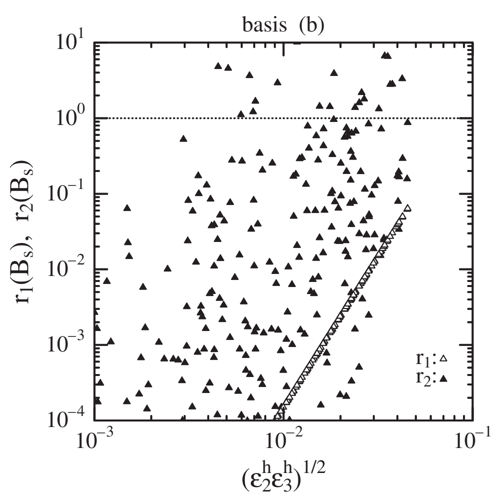

FIG. 4. Scatter plots of $r_1(B_s) \equiv |C^1_{B_s}|/|C^1_{B_s}|_{\max}$ (△) and $r_2(B_s) \equiv |C^2_{B_s}|/|C^2_{B_s}|_{\max}$ (▲) versus $(\epsilon_2^h\epsilon_3^h)^{1/2}$ for the B_s-$\bar{B}_s$ mixing, similarly to Fig. 3.

IV. DECAYS OF SINGLET QUARKS AND HIGGS PARTICLES

We now investigate the decays of the singlet quarks and Higgs particles, which will provide distinct signatures upon their productions at the LHC. The flavor-changing interactions between the singlet quarks Q and the ordinary quarks q are relevant for these decays at the tree level. Specifically, the left-handed Z-boson couplings are given as

$$Z_{\mathcal{Q}}[q^\dagger Q]_{ia} = Z_{\mathcal{Q}}[Q^\dagger q]^*_{ai} = (V^\dagger_{q_L}\epsilon_{q_L})_{ia} \simeq (\epsilon_{q_L})_{ia}, \quad (51)$$

while the right-handed ones are absent. Note here that $Z_{\mathcal{Q}}[q^\dagger Q] = \Delta Z_{\mathcal{Q}}[q^\dagger Q]$, as shown in Eq. (A7); the q-Q transitions in the Z-boson couplings are just induced as the q-Q mixing effect. The left-handed W-boson couplings are given in terms of the Z-boson couplings and the CKM matrix in a good approximation up to the second order of the small q-Q mixing as

$$\mathcal{V}[u^\dagger D]_{ia} = \mathcal{V}[D^\dagger u]^*_{ai} \simeq (V\mathcal{Z}_{\mathcal{D}}[d^\dagger D])_{ia}, \tag{52}$$

$$\mathcal{V}[d^\dagger U]_{ia} = \mathcal{V}[U^\dagger d]^*_{ai} \simeq (V^\dagger \mathcal{Z}_{\mathcal{U}}[u^\dagger U])_{ia}, \tag{53}$$

while the right-handed ones are absent. The neutral scalar couplings are given as

$$\Lambda^H_{\mathcal{Q}}[q^c Q]_{ia} = (m_{q_i}/v)\mathcal{Z}_{\mathcal{Q}}[q^\dagger Q]_{ia}, \tag{54}$$

$$\Lambda^H_{\mathcal{Q}}[Q^c q]_{ai} = (m_{Q_a}/v)\mathcal{Z}_{\mathcal{Q}}[Q^\dagger q]_{ai}, \tag{55}$$

$$\Lambda^{S_+}_{\mathcal{Q}}[q^c Q]_{ia} = -(m_{q_i}/v_S)\mathcal{Z}_{\mathcal{Q}}[q^\dagger Q]_{ia}, \tag{56}$$

$$\Lambda^{S_+}_{\mathcal{Q}}[Q^c q]_{ai} = -(m_{Q_a}/v_S)\mathcal{Z}_{\mathcal{Q}}[Q^\dagger q]_{ai}, \tag{57}$$

$$\Lambda^{S_-}_{\mathcal{Q}}[q^c Q]_{ia} = (V^\dagger_{q_{\rm R}} f^-_Q V_{Q_{\rm L}} - \epsilon'_{q_{\rm R}}\lambda^-_Q V_{Q_{\rm L}})_{ia}/\sqrt{2}, \tag{58}$$

$$\Lambda^{S_-}_{\mathcal{Q}}[Q^c q]_{ai} = (-\epsilon^\dagger_{q_{\rm R}} f^-_Q \epsilon'^\dagger_{q_{\rm L}} - V^\dagger_{Q_{\rm R}}\lambda^-_Q \epsilon'^\dagger_{q_{\rm L}})_{ai}/\sqrt{2}. \tag{59}$$

Here, $\Lambda^{\phi^0_r}_{\mathcal{Q}}[q^c Q]_{ia}$ stands for $\bar{q}_{i\rm R}Q_{a\rm L}\phi^0_r$, and $\Lambda^{\phi^0_r}_{\mathcal{Q}}[Q^c q]_{ai}$ for $\bar{Q}_{a\rm R}q_{i\rm L}\phi^0_r$, respectively, in terms of the Dirac fields. The relations among the gauge and scalar couplings in Eqs. (51)–(57) are derived in the Appendix.

A. Singlet quark decays

We first investigate the singlet quark decays. We describe the essential features by considering the case of one down-type singlet quark D ($a = 1$ is omitted for $N_D = 1$ and $N_U = 0$). Similar results are obtained in the general cases of some D and U quarks, especially for the lightest singlet quark. While the heavier singlet quarks may decay dominantly into the lighter singlet quarks and Higgs particles in the general cases, we concentrate on the decays of the lightest singlet quark producing the ordinary quarks.

The partial widths of the relevant decay modes are calculated (when they are kinematically allowed) as

$$\Gamma(D \to u_i W) = \frac{G_F}{\sqrt{2}}\frac{m_D^3}{8\pi} g(x_W, x_{u_i})|\mathcal{V}[u^\dagger D]_i|^2, \tag{60}$$

$$\Gamma(D \to d_i Z) = \frac{G_F}{\sqrt{2}}\frac{m_D^3}{16\pi}(1 - 3x_Z^4 + 2x_Z^6)|\mathcal{Z}_{\mathcal{D}}[d^\dagger D]_i|^2, \tag{61}$$

$$\Gamma(D \to d_i H) = \frac{m_D}{16\pi}(1 - x_H^2)^2(|\Lambda^H_{\mathcal{D}}[D^c d]_i|^2 + |\Lambda^H_{\mathcal{D}}[d^c D]_i|^2), \tag{62}$$

$$\Gamma(D \to d_i S_\pm) = \frac{m_D}{16\pi}(1 - x_{S_\pm}^2)^2(|\Lambda^{S_\pm}_{\mathcal{D}}[D^c d]_i|^2 + |\Lambda^{S_\pm}_{\mathcal{D}}[d^c D]_i|^2), \tag{63}$$

where $x_W = m_W/m_D$, $x_Z = m_Z/m_D$, $x_H = m_H/m_D$, $x_{S_\pm} = m_{S_\pm}/m_D$, $x_{u_i} = m_{u_i}/m_D$, and

$$g(x, y) = [1 - (x + y)^2]^{1/2}[1 - (x - y)^2]^{1/2} \times [x^2(1 - 2x^2 + y^2) + (1 - y^2)^2]. \tag{64}$$

The scalar mixing is neglected ($O_\phi = \mathbf{1}$) for a while. The kinematic effects of $m_{d_i}/m_D \lesssim 0.02$ for $m_D \gtrsim 200$ GeV may be neglected in a good approximation, while $\Gamma(D \to tW)$ depends sensibly on m_t/m_D.

The flavor structure of the d-D mixing is measured manifestly in the D decays into the ordinary quarks $d_i = d, s, b$ and the Z boson as

$$\Gamma(D \to d_i Z) \propto |(\epsilon_{d_{\rm L}})_i|^2, \tag{65}$$

where $\mathcal{Z}_{\mathcal{D}}[d^\dagger D]_i \simeq (\epsilon_{d_{\rm L}})_i$ for the Z-boson coupling. The partial width of the D quark decays producing the Z boson is inclusively estimated for the reference as

$$\Gamma_D(Z) \equiv \sum_i \Gamma(D \to d_i Z) \sim 20\ \text{MeV} \times \left(\frac{m_D}{500\ \text{GeV}}\right)^3 \frac{|\epsilon^h|^2}{(0.03)^2}, \tag{66}$$

where $(\epsilon_{d_{\rm L}})_i \sim \epsilon^h_i$ with $|\epsilon^h| \equiv [(\epsilon^h_1)^2 + (\epsilon^h_2)^2 + (\epsilon^h_3)^2]^{1/2}$ in the basis (b), and $\epsilon^h_i \to (m_{d_i}/m_D)\epsilon^f_i$ for $(\epsilon_{d_{\rm L}})_i$ in the basis (a). By considering Eqs. (51), (52), (54), and (55) with $|\Lambda^H_{\mathcal{D}}[d^c D]_i|^2/|\Lambda^H_{\mathcal{D}}[D^c d]_i|^2 = (m_{d_i}/m_D)^2 \ll 1$, we find the well-known relations [32]

$$\Gamma(D \to u_i W) \sim 2\Gamma(D \to d_i Z), \tag{67}$$

$$\Gamma(D \to d_i H) \sim \Gamma(D \to d_i Z), \tag{68}$$

or inclusively

$$\Gamma_D(W) \equiv \sum_i \Gamma(D \to u_i W) \sim 2\Gamma_D(Z), \tag{69}$$

$$\Gamma_D(H) \equiv \sum_i \Gamma(D \to d_i H) \sim \Gamma_D(Z), \tag{70}$$

where $O_\phi = \mathbf{1}$. The actual values of these widths are evaluated depending on the kinematic factors and the CKM mixing.

In the present model with the complex singlet Higgs, the decays of the singlet quark D producing the singlet Higgs scalars $S_\pm$ are possible for $m_D > m_{S_\pm} + m_{d_i}$. Especially, it is remarkable that the decays with S_- may dominate over the other decay modes. By considering $(f^-_D)_i \sim (\epsilon'_{d_{\rm R}})_i\lambda^-_D \sim (m_D/v_S)\epsilon^f_i$ and $\lambda^-_D(\epsilon'^\dagger_{d_{\rm L}})_i \sim (m_D/v_S)\epsilon^h_i$ in

Eqs. (58) and (59), the S_- couplings are estimated roughly as

$$\Lambda_{\mathcal{D}}^{S_-}[d^c D]_i \sim (m_D/v_S)\epsilon_i^f, \tag{71}$$

$$\Lambda_{\mathcal{D}}^{S_-}[D^c d]_i \sim (m_D/v_S)\epsilon_i^h. \tag{72}$$

Here, for the sake of convenience we adopt $\epsilon_i^h = (m_{d_i}/m_D)\epsilon_i^f$ in the basis (a) though $h_d = \mathbf{0}$, while $\epsilon_i^f = (v_S/m_D)|2(f_Q)_i|/\sqrt{2}$ in the basis (b) though $f_Q^+ = \mathbf{0}$, as discussed concerning Eq. (35). Then, we estimate roughly the partial width of the D decays producing S_- as

$$\Gamma_D(S_-) \equiv \sum_i \Gamma(D \to d_i S_-) \sim 10\,\mathrm{MeV} \times \left(\frac{m_D}{500\,\mathrm{GeV}}\right)^3 \left(\frac{500\,\mathrm{GeV}}{v_S}\right)^2 \frac{|\epsilon^f|^2 + |\epsilon^h|^2}{(0.03)^2}, \tag{73}$$

where $|\epsilon^f| \equiv [(\epsilon_1^f)^2 + (\epsilon_2^f)^2 + (\epsilon_3^f)^2]^{1/2}$. (The actual value is reduced to some extent by the kinematic factor for $m_D \sim m_{S_-}$.) This width $\Gamma_D(S_-)$ for the decays into the singlet scalar S_- dominates over the reference width $\Gamma_D(Z)$ for the decays into the Z boson in Eq. (66) for $|\epsilon^f|^2 \gg |\epsilon^h|^2$, especially in the basis (a) with $\epsilon_i^h \to (m_{d_i}/m_D)\epsilon_i^f$. As for the D decays with S_+, the partial width is simply related to $\Gamma_D(Z)$ by Eq. (57) as

$$\Gamma_D(S_+) \equiv \sum_i \Gamma(D \to d_i S_+) \sim (v/v_S)^2 \Gamma_D(Z), \tag{74}$$

which amounts to $O(10\%)$ of $\Gamma_D(Z)$ for $v_S \approx 500$ GeV. Even this slight enhancement due to $\Gamma_D(S_+)$ for the D decays into the scalars H and S_+ might serve as an experimental signature for the singlet Higgs even if S_- is absent in the model with one real $S \equiv S_+$.

Here, it should be noted that the S_- coupling may even provide significant contributions to the decays $D \to d_i H$ through the H-S_- mixing ϵ_{HS_-} in O_ϕ. In fact, the d-D coupling with the standard Higgs H (more precisely the mass eigenstate $\phi_1 \simeq H$ with $\epsilon_{HS_-} \ll 1$) is replaced in Eq. (62) as

$$\Lambda_{\mathcal{D}}^H \to \Lambda_{\mathcal{D}}^H + \epsilon_{HS_-}\Lambda_{\mathcal{D}}^{S_-}. \tag{75}$$

Then, instead of Eq. (70) we obtain

$$\Gamma_D(H) \sim \Gamma_D(Z) + \epsilon_{HS_-}^2 \Gamma_D(S_-), \tag{76}$$

where the interference term between $\Lambda_{\mathcal{D}}^H$ and $\Lambda_{\mathcal{D}}^{S_-}$ is omitted for simplicity. This enhancement of $\Gamma_D(H)$ with $\epsilon_{HS_-}\Lambda_{\mathcal{D}}^{S_-}$ in Eq. (75) is valid even when the decays $D \to d_i S_-$ are forbidden kinematically for $m_D < m_{S_-} + m_{d_i}$. In the presence of a small but sizable H-S_- mixing $\epsilon_{HS_-} \sim 0.01$–$0.1$ the singlet quark decays $D \to d_i H$ may become the dominant modes, particularly in the basis (a) due to the substantial suppression of $D \to d_i Z$ with $|Z_{\mathcal{D}}[d^\dagger D]_i|^2 \sim (m_{d_i}/m_D)^2(\epsilon_i^f)^2 \lesssim 10^{-4}$. Hence, if $\Gamma_D(H) \gg \Gamma_D(Z)$ is confirmed experimentally, which is contrary to the usual expectation of Eq. (70), it will provide a distinct evidence for the complex singlet Higgs field S with the H-S_- mixing. The decays $D \to d_i S_+$ may also be enhanced substantially as $\Gamma_D(S_+) \sim \epsilon_{S_+S_-}^2 \Gamma_D(S_-)$ via a sizable S_+-S_- mixing $\epsilon_{S_+S_-}$.

We present in the following the detailed estimates on the widths of the relevant decay modes, where the constraints on the d-D mixing from the $\Delta F = 2$ meson mixings and the diagonal Z-boson couplings are checked to be satisfied according to the numerical calculations performed in Sec. III.

We suitably denote the ratios of the relevant widths to the reference width as

$$R_D(X/Z) \equiv \frac{\Gamma_D(X)}{\Gamma_D(Z)}, \tag{77}$$

where $X = W, H, S_+, S_-$. For the usual decay modes $D \to u_i W$, $D \to d_i Z$ and $D \to d_i H$, scatter plots of $R_D(W/Z)$ (□, ■) and $R_D(H/Z)$ (△, ▲) versus the singlet quark mass m_D are shown in Fig. 5 for the bases (a) (□, △) and (b) (■, ▲). Here, $v_S = 500$ GeV, and the Higgs scalar mixing is assumed to be absent ($O_\phi = \mathbf{1}$). Similar results are obtained for the bases (a) and (b) since these bases are equivalently related to each other by the unitary transformation, as discussed in Sec. II. Note here that larger values may be obtained for the singlet quark mass m_D with a given singlet Higgs VEV v_S in the basis (a) (□, △), which is due to the significant contribution of the q-Q mixing term $\Delta_{qQ} = f_Q^+ v_S/\sqrt{2}$ for $|\epsilon^f| \sim 1$. The lower boundary curve for $R_D(W/Z)$ reflects the kinematic factor

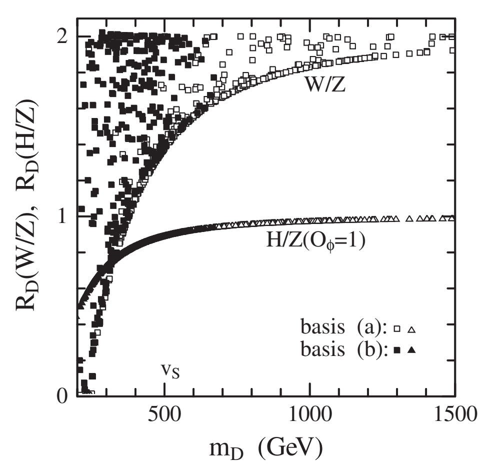

FIG. 5. $R_D(W/Z) \equiv \Gamma_D(W)/\Gamma_D(Z)$ versus m_D is shown for the bases (a) (□) and (b) (■). $R_D(H/Z) \equiv \Gamma_D(H)/\Gamma_D(Z)$ versus m_D is also shown for the bases (a) (△) and (b) (▲). Here, $v_S = 500$ GeV, and the Higgs scalar mixing is assumed to be absent ($O_\phi = \mathbf{1}$).

of the dominant top contribution $D \to tW$ with $|\mathcal{V}[u^\dagger D]_3|^2 \gg |\mathcal{V}[u^\dagger D]_{1,2}|^2$. In this case the singlet D quark mixes mainly with the b quark as $|(\epsilon_{d_L})_3|^2 \gg |(\epsilon_{d_L})_{1,2}|^2$. On the other hand, in the case that the top contribution is negligible with $|\mathcal{V}[u^\dagger D]_3|^2 \ll |\mathcal{V}[u^\dagger D]_{1,2}|^2$, the asymptotic value $R_D(W/Z) = 2$ is almost saturated for $m_D \gtrsim 300$ GeV. We also see that $R_D(H/Z)$ approaches the asymptotic value $R_D(H/Z) = 1$ showing the kinematic dependence on m_D. These results really confirm the usual expectation in Eqs. (69) and (70). It should, however, be remarked that as shown in Eq. (76), the D decays with the standard Higgs H may be enhanced substantially as $R_D(H/Z) \gg 1$ due to the singlet Higgs coupling $\Lambda_{\mathcal{D}}^{S_-}$ via the H-S_- mixing.

The reference width $\Gamma_D(Z)$ versus the magnitude of the left-handed d-D mixing $|\epsilon^h|$, as given in Eq. (66), is shown in Fig. 6. Here, the marks ○ and ● denote the estimates in the bases (a) and (b), respectively, and $\epsilon_i^h = (m_{q_i}/m_D)\epsilon_i^f$ as Eq. (35) is adopted in the basis (a) though $\epsilon_i^h = 0$ formally. This plot of $\Gamma_D(Z)$ spreads according to the variation of $m_D \sim 100$ GeV–1 TeV due to the fact that $\Gamma_D(Z)$ is almost proportional to m_D^3.

The decay widths $\Gamma_D(Z)$ and $\Gamma_D(S_-)$ for the significant modes are compared in Fig. 7. According to Eqs. (66) and (73), by measuring these decay widths we can estimate the magnitudes of d-D mixings, $|\epsilon^h|$ from the h_d coupling and $|\epsilon^f|$ from the f_D and f_D' couplings. Specifically, $\Gamma_D(S_-) \gg \Gamma_D(Z)$ for $|\epsilon^f| \gg |\epsilon^h|$ as in the basis (a) (○), while $\Gamma_D(S_-) \lesssim \Gamma_D(Z)$ for $|\epsilon^f| \lesssim |\epsilon^h|$ as in the basis (b) (●). The decay width $\Gamma_D(H)$ with the standard Higgs H is also relevant to measure the relative significance of $|\epsilon^h|$ versus $|\epsilon^f|$ according to Eq. (76) with the sizable H-S_- mixing. This is useful even if the decays $D \to d_i S_-$ are kinematically forbidden for $m_{S_-} > m_D + m_{d_i}$. A plot of $R_D(H/Z)$ versus $|\epsilon^f|/|\epsilon^h|$ is shown in Fig. 8 for the bases (a) (△) and (b) (▲), where $\epsilon_{HS_-} = 0.1$ is taken typically for the H-S_- mixing. In the region of $|\epsilon^f|/|\epsilon^h| \gg 1$, the contribution of the singlet Higgs coupling $\Lambda_{\mathcal{D}}^{S_-}$ dominates as $\Gamma_D(H) \sim \epsilon_{HS_-}^2 \Gamma_D(S_-) \gg \Gamma_D(Z)$. On the other hand, in the region of $|\epsilon^f|/|\epsilon^h| \lesssim 1$ we have $\Gamma_D(H) \sim \Gamma_D(Z)$ as usually expected.

In these plots of Figs. 5–8, the regions for the bases (a) and (b) overlap as expected, but they are not identical. This is because the actual parameter ranges are somewhat different for the bases (a) and (b); although the parameter ranges have been taken apparently in the same way for these bases in the numerical calculations, except that $h_q = \mathbf{0}$ in the basis (a), they are not mapped identically to each other by the unitary transformation between the bases (a) and (b). Specifically, in the basis (a) we have a significant constraint $|\epsilon^h|/|\epsilon^f| \lesssim m_b/m_D \sim 0.01$ from the relation $\epsilon_i^h \sim (m_{d_i}/m_D)\epsilon_i^f$, implying $|\epsilon^h| \lesssim 0.01$ as long as $|\epsilon^f| \lesssim 1$. This is explicitly seen in Figs. 6 and 8. We also note that the plot for the basis (a) in Fig. 8 spreads significantly. This is in some sense an artifact due to the definition of the d-D mixing parameters ϵ_i^f in terms of $f_D^+ \equiv f_D + f_D'$ for the basis (a). The singlet S_- coupling $\Lambda_{\mathcal{D}}^{S_-}$ is rather given by $f_D^- \equiv i(f_D - f_D')$. The spread in the plot for the basis (a) really reflects the partial cancellation between f_D and f_D' for the $\Lambda_{\mathcal{D}}^{S_-}$ coupling. On the other hand, for the basis (b) the parameters ϵ_i^f are defined suitably with $f_D^- = 2if_D$ ($f_D = -f_D'$ for $f_D^+ = \mathbf{0}$). Hence, the plot for the basis (b) almost lies on a curve up to the small fluctuation due to the kinematic factor, which gives the boundary of the plot for the basis (a). This boundary really corresponds to the extreme case $f_D \approx -f_D'$ for $|f_D^-| \approx 2|f_D|$ in the basis (a).

As seen so far, the singlet D quark decays present us important insights on the d-D mixing effects for the flavor-changing processes. Especially, if it is observed that $\Gamma_D(S_-) \gg \Gamma_D(Z)$, we find that the singlet Higgs scalar

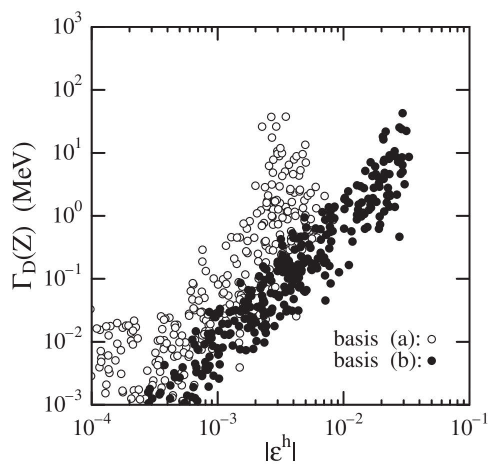

FIG. 6. $\Gamma_D(Z)$ versus $|\epsilon^h|$ in the bases (a) (○) and (b) (●). Here, $\epsilon_i^h = (m_{q_i}/m_D)\epsilon_i^f$ as Eq. (35) is adopted in the basis (a) though $\epsilon_i^h = 0$ formally.

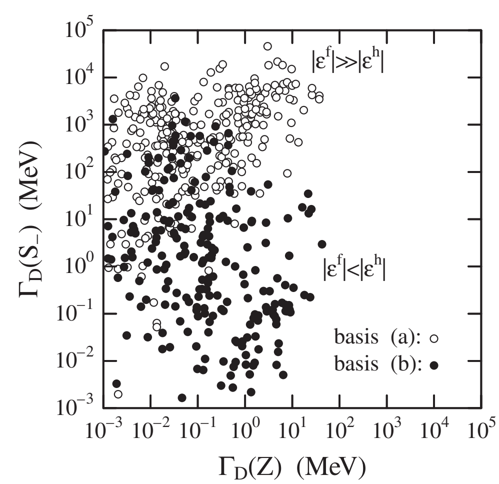

FIG. 7. $\Gamma_D(Z)$ and $\Gamma_D(S_-)$ are compared in the bases (a) (○) and (b) (●).

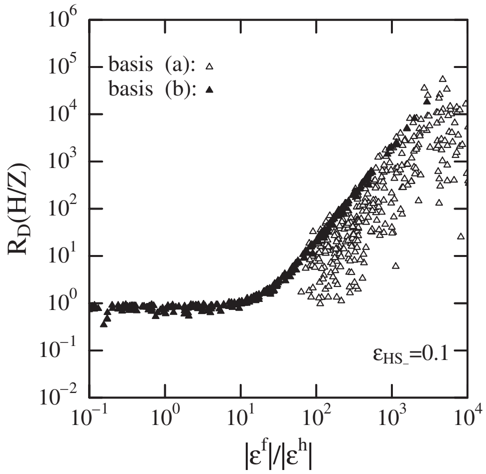

FIG. 8. $R_D(H/Z) \equiv \Gamma_D(H)/\Gamma_D(Z)$ versus $|\epsilon^f|/|\epsilon^h|$ is shown for the bases (a) (△) and (b) (▲), where $\epsilon_{HS_-} = 0.1$ is taken typically for the H-S_- mixing.

interactions dominate over the Z-boson interactions. For example, suppose that the current experimental bound for the B_d-$\bar{B}_d$ mixing [39] is almost saturated with $(\epsilon_1^f \epsilon_3^f)^{1/2} \sim 0.2$ for $m_{S_-} \sim 300$ GeV in the basis (a) as shown in Eq. (42), which implies $|\epsilon^f| \gtrsim \sqrt{2} \times 0.2 \gg |\epsilon^h|$. Then, we expect $\Gamma_D(S_-) \sim 1$ GeV–10 GeV $\gg \Gamma_D(Z)$ for $m_D \sim 500$ GeV–1 TeV, as seen in Eq. (73) and Fig. 7. Contrarily, if $\Gamma_D(S_-) \lesssim 1$ MeV for $m_D \gtrsim 500$ GeV, which implies $|\epsilon^f| \lesssim 0.01$, the scalar FCNC's do not provide significant contributions to the $\Delta F = 2$ meson mixings. As for the D decays with the Z boson, if there is a significant left-handed d-D mixing as $|\epsilon^h| \sim 0.03$ in the basis (b), we expect $\Gamma_D(Z) \sim 10$ MeV–100 MeV for $m_D \sim 500$ GeV–1 TeV in Eq. (66). In this case, the bound for the B_d-$\bar{B}_d$ mixing may be saturated by the Z-mediated FCNC with $(\epsilon_1^h \epsilon_3^h)^{1/2} \sim 0.03$, as shown in Eq. (44). On the other hand, if $\Gamma_D(Z) \lesssim 0.01$ MeV for $m_D \gtrsim 500$ GeV, which implies $|\epsilon^h| \lesssim 0.001$ (see Fig. 6), the effects of the Z-mediated FCNC's are negligible in the $\Delta F = 2$ meson mixings.

B. Higgs particle decays

We next survey the decays of the Higgs particles H, S_+ and S_-, or more precisely the mass eigenstates ϕ_1, ϕ_2, ϕ_3 with the mixing matrix O_ϕ.

The standard Higgs H is probably lighter than the singlet quarks Q ($m_Q > m_H \approx 120$ GeV) so that its decays involving the singlet quarks are forbidden kinematically. It should also be noted that the q-Q mixing effect on the H coupling with the ordinary quarks appears merely at the second order related to the modification of the Z-boson coupling, as seen in Eq. (31). Hence, the Higgs particle H will decay essentially in the same way as the standard model unless the H-S_- mixing is so large as to provide significant effects.

The singlet Higgs particles $S_\pm$ will be produced significantly by gluon fusion via a loop of singlet quark Q coupled to $S_\pm$ with the strength $\sim |\lambda_Q^\pm| \sim m_Q/v_S \sim 1$. The production rates of $S_\pm$ will be comparable to that of the standard Higgs H unless $S_\pm$ are substantially heavier than H. If $m_{S_\pm} < m_Q$, the singlet quark decays $Q \to q_i S_\pm$ also produce $S_\pm$, as discussed so far. It should be remarked that some indirect indication for the presence of S_- may be obtained via the H-S_- mixing, specifically in the case of $\Gamma_Q(H) \gg \Gamma_Q(Z)$ for the singlet quark decays $Q \to qH$.

In the case of $m_{S_\pm} < m_Q$, the singlet Higgs particles $S_\pm$ decay predominantly into the ordinary quarks through the scalar interactions in Eqs. (32)–(34) at the second order of the q-Q mixing:

$$S_\pm \to q_i \bar{q}_j. \tag{78}$$

The decay widths are estimated particularly for S_- in comparison with that of the standard Higgs H as

$$\begin{aligned} \frac{\Gamma(S_- \to q_i \bar{q}_j)}{\Gamma(H \to b\bar{b})} &\sim \frac{m_{S_-}(|\Lambda_Q^{S_-}[q^c q]_{ij}|^2 + |\Lambda_Q^{S_-}[q^c q]_{ji}|^2)}{m_H |\Lambda_Q^H [q^c q]_{33}|^2} \\ &\sim [(m_{S_-}/m_H)(m_Q/v_S)^2/(m_b/v)^2] \\ &\quad \times [(\epsilon_i^f)^2(\epsilon_j^h)^2 + (\epsilon_j^f)^2(\epsilon_i^h)^2], \end{aligned} \tag{79}$$

where $\epsilon_j^h \to (m_{q_j}/m_Q)\epsilon_j^f$ in the basis (a). We estimate, for instance, $\Gamma(S_- \to b\bar{b})/\Gamma(H \to b\bar{b}) \sim [10(\epsilon_3^f \epsilon_3^h)^{1/2}]^4$ for $m_{S_-}/m_H \sim 3$, $m_D/v_S \sim 1$ and $m_b/v \simeq 1/60$, which may amount to $O(1)$ for the large b-D mixing as $\epsilon_3^f \sim 1$ and $\epsilon_3^h \sim (m_b/m_D)\epsilon_3^f \sim 0.01$. The flavor-changing decays such as $S_- \to b\bar{s}$ as well as the flavor-diagonal ones may have significant fractions. This is distinct from the standard Higgs H, presenting a promising signature of the singlet Higgs S_-. In fact, we estimate

$$\frac{\Gamma(S_- \to b\bar{d}_j)}{\Gamma(S_- \to b\bar{b})} \sim (\epsilon_j^f/\epsilon_3^f)^2 + (\epsilon_j^h/\epsilon_3^h)^2, \tag{80}$$

depending on the flavor structure of the d-D mixing. If the singlet U quarks are present with a large t-U mixing, the decays $S_- \to t\bar{t}$, $t\bar{u}_i$, $u_i\bar{t}$ involving the top quark may be observed with significant fractions.

In this way, the decays of the singlet Higgs S_- into the ordinary quarks are determined in terms of the q-Q mixing parameters with close connection to the flavor-changing processes such as the $\Delta F = 2$ meson mixings. As for the singlet Higgs S_+, its coupling is given in Eq. (32) by the Z-boson coupling at the second order of q-Q mixing with further suppression by the ordinary quark mass. These arguments on the $S_\pm$ couplings with the ordinary quarks generally suggest that

$$\Gamma_H \gtrsim \Gamma_{S_-} \gg \Gamma_{S_+}(m_{S_\pm} < m_Q, O_\phi \approx \mathbf{1}) \tag{81}$$

for the decay rates of the Higgs particles if the Higgs mixing is negligibly small. It is, however, possible that the large Higgs mixing, in cooperation with the q-Q mixing, affects significantly the decays of H and $S_\pm$. (See also Ref. [44] for investigations of extended Higgs models at the LHC.) Therefore, the observations of the Higgs particle decays present important information on the Higgs mixing and q-Q mixing.

In the case of $m_{S_\pm} > m_Q$, the singlet quark decays $Q \to qS_\pm$ are forbidden kinematically. Even in such a case the singlet Higgs $S_\pm$ will be produced significantly by the gluon fusion via the singlet quark loop. Then, they decay predominantly involving the singlet quarks as

$$S_\pm \to Q\bar{q}, \bar{Q}q, Q\bar{Q}. \tag{82}$$

The decay widths are estimated in terms of the scalar couplings $\Lambda_Q^{S_\pm}$ in Eq. (27). In particular, if $m_{S_\pm} > 2m_Q$ we have

$$\Gamma(S_\pm \to Q\bar{Q}) \sim \frac{(m_Q/v_S)^2 m_{S_\pm}}{16\pi} \gtrsim 10 \text{ GeV} \gg \Gamma_H \tag{83}$$

with $\mathrm{Br}(S_\pm \to Q\bar{Q}) \approx 1$ for $m_{S_\pm} \gtrsim 500$ GeV and $|\lambda_Q^\pm| \sim m_Q/v_S \sim 1$.

V. SUMMARY

The singlet quarks in cooperation with the single Higgs field may provide various interesting effects in particle physics and cosmology through the mixing with the ordinary quarks (q-Q mixing). It is hence worth considering their phenomenological implications toward the discovery of them at the LHC. In this study we have investigated the flavor-changing interactions in the model with singlet quarks and singlet Higgs, which are induced by the q-Q mixing. While the gauge interactions have been investigated extensively in the literature, we have rather noted here that the scalar interactions mediated by the singlet Higg may provide significant effects in some cases. This possibility has not been paid so much attention before in the models with singlet quarks. We have considered the effects of the gauge and scalar interactions in the $\Delta F = 2$ mixings of the neutral mesons to show the currently allowed range of the q-Q mixing. Then, we have investigated the decays of the singlet quarks and Higgs particles as the new physics around the electroweak scale to the TeV scale, which is accessible to the LHC. Especially, the right-handed q-Q mixing may be tolerably large without contradicting the current bounds on the flavor-changing processes, since it is not involved directly in the electroweak gauge interactions. If this is the case, the scalar coupling by the singlet Higgs, and possibly through the Higgs mixing, provides distinct signatures for the decays of the singlet quarks and Higgs particles, which should be compared with the conventionally expected ones via the gauge and standard Higgs couplings. We expect that observations of the singlet quarks and Higgs particles will present us important insights on the q-Q mixing and Higgs mixing.

ACKNOWLEDGMENTS

We would like to thank M. Senami for valuable discussions.

APPENDIX: RELATIONS AMONG THE GAUGE AND SCALAR COUPLINGS

We here derive the suitable relations among the gauge and scalar couplings.

The full mixing matrix for the left-handed W-boson coupling is given by

$$\mathcal{V} = \mathcal{V}_{\mathcal{U}_\mathrm{L}}^\dagger \begin{pmatrix} V_0 & \mathbf{0} \\ \mathbf{0} & \mathbf{0} \end{pmatrix} \mathcal{V}_{\mathcal{D}_\mathrm{L}} = \begin{pmatrix} V_{u_\mathrm{L}}^\dagger V_0 V_{d_\mathrm{L}} & V_{u_\mathrm{L}}^\dagger V_0 \epsilon_{d_\mathrm{L}} \\ \epsilon_{u_\mathrm{L}}^\dagger V_0 V_{d_\mathrm{L}} & \epsilon_{u_\mathrm{L}}^\dagger V_0 \epsilon_{d_\mathrm{L}} \end{pmatrix}. \tag{A1}$$

Then, we obtain from the off-diagonal blocks

$$\mathcal{V}[u^\dagger D] = V_{u_\mathrm{L}}^\dagger V_0 \epsilon_{d_\mathrm{L}} \simeq V V_{d_\mathrm{L}}^\dagger \epsilon_{d_\mathrm{L}}, \tag{A2}$$

$$\mathcal{V}[U^\dagger d] = \epsilon_{u_\mathrm{L}}^\dagger V_0 V_{d_\mathrm{L}} \simeq \epsilon_{u_\mathrm{L}}^\dagger V_{u_\mathrm{L}} V, \tag{A3}$$

where the approximate unitarity $V_{q_\mathrm{L}} V_{q_\mathrm{L}}^\dagger \simeq \mathbf{1}$ is considered up to the second order of the small q-Q mixing. By applying Eq. (51) for the Z-boson coupling to Eqs. (A2) and (A3), we obtain Eqs. (52) and (53).

The left-handed Z-boson coupling is given originally in the electroweak basis (q_0, Q_0) as

$$\mathcal{Z}_Q^{(0)} = \begin{pmatrix} \mathbf{1} & \mathbf{0} \\ \mathbf{0} & \mathbf{0} \end{pmatrix} - a \begin{pmatrix} \mathbf{1} & \mathbf{0} \\ \mathbf{0} & \mathbf{1} \end{pmatrix}, \tag{A4}$$

where $a = \sin^2\theta_W Q_\mathrm{em}(\mathcal{Q})/I_3(q_0)$, and the division by $I_3(q_0) = \pm 1/2$ is for convenience of notation. It is transformed in the basis of mass eigenstates (q, Q) as

$$\begin{aligned} \mathcal{Z}_Q &= \mathcal{V}_{\mathcal{Q}_\mathrm{L}}^\dagger \mathcal{Z}_Q^{(0)} \mathcal{V}_{\mathcal{Q}_\mathrm{L}} \\ &= \mathcal{V}_{\mathcal{Q}_\mathrm{L}}^\dagger \begin{pmatrix} \mathbf{1} & \mathbf{0} \\ \mathbf{0} & \mathbf{0} \end{pmatrix} \mathcal{V}_{\mathcal{Q}_\mathrm{L}} - a \begin{pmatrix} \mathbf{1} & \mathbf{0} \\ \mathbf{0} & \mathbf{1} \end{pmatrix}. \end{aligned} \tag{A5}$$

The modification of the Z-boson coupling due to the q-Q mixing is calculated from Eqs. (A4) and (A5) as

$$\begin{aligned} \Delta \mathcal{Z}_Q = \mathcal{Z}_Q - \mathcal{Z}_Q^{(0)} &= \mathcal{V}_{\mathcal{Q}_\mathrm{L}}^\dagger \begin{pmatrix} \mathbf{1} & \mathbf{0} \\ \mathbf{0} & \mathbf{0} \end{pmatrix} \mathcal{V}_{\mathcal{Q}_\mathrm{L}} - \begin{pmatrix} \mathbf{1} & \mathbf{0} \\ \mathbf{0} & \mathbf{0} \end{pmatrix} \\ &= \begin{pmatrix} -\epsilon'_{q_\mathrm{L}} \epsilon'^\dagger_{q_\mathrm{L}} & V_{q_\mathrm{L}}^\dagger \epsilon_{q_\mathrm{L}} \\ \epsilon_{q_\mathrm{L}}^\dagger V_{q_\mathrm{L}} & \epsilon_{q_\mathrm{L}}^\dagger \epsilon_{q_\mathrm{L}} \end{pmatrix}. \end{aligned} \tag{A6}$$

Here, we have considered the relation $V_{q_\mathrm{L}}^\dagger V_{q_\mathrm{L}} - \mathbf{1} = -\epsilon'_{q_\mathrm{L}} \epsilon'^\dagger_{q_\mathrm{L}}$ from the unitarity of $\mathcal{V}_{\mathcal{Q}_\mathrm{L}}$ to obtain Eq. (22) for the upper diagonal block $\Delta \mathcal{Z}_Q[q^\dagger q]$ in $\Delta \mathcal{Z}_Q$. We also obtain the Z boson q-Q couplings in Eq. (51) from the off-diagonal blocks in Eqs. (A5) and (A6) as

$$\mathcal{Z}_Q[q^\dagger Q] = \Delta \mathcal{Z}_Q[q^\dagger Q] = V^\dagger_{q_L} \epsilon_{q_L} = (\mathcal{Z}_Q[Q^\dagger q])^\dagger. \tag{A7}$$

We note the relation from Eq. (A6) as

$$\mathcal{V}^\dagger_{Q_L} \begin{pmatrix} \mathbf{1} & \mathbf{0} \\ \mathbf{0} & \mathbf{0} \end{pmatrix} \mathcal{V}_{Q_L} = \Delta \mathcal{Z}_Q + \begin{pmatrix} \mathbf{1} & \mathbf{0} \\ \mathbf{0} & \mathbf{0} \end{pmatrix}. \tag{A8}$$

By taking the difference between this relation and that for the unit matrix

$$\mathcal{V}^\dagger_{Q_L} \begin{pmatrix} \mathbf{1} & \mathbf{0} \\ \mathbf{0} & \mathbf{1} \end{pmatrix} \mathcal{V}_{Q_L} = \begin{pmatrix} \mathbf{1} & \mathbf{0} \\ \mathbf{0} & \mathbf{1} \end{pmatrix}, \tag{A9}$$

we obtain another relation

$$\mathcal{V}^\dagger_{Q_L} \begin{pmatrix} \mathbf{0} & \mathbf{0} \\ \mathbf{0} & \mathbf{1} \end{pmatrix} \mathcal{V}_{Q_L} = -\Delta \mathcal{Z}_Q + \begin{pmatrix} \mathbf{0} & \mathbf{0} \\ \mathbf{0} & \mathbf{1} \end{pmatrix}. \tag{A10}$$

By using Eq. (A8), we calculate

$$\begin{aligned} \mathcal{V}^\dagger_{Q_R} \mathcal{M}_Q \begin{pmatrix} \mathbf{1} & \mathbf{0} \\ \mathbf{0} & \mathbf{0} \end{pmatrix} \mathcal{V}_{Q_L} &= \bar{\mathcal{M}}_Q \mathcal{V}^\dagger_{Q_L} \begin{pmatrix} \mathbf{1} & \mathbf{0} \\ \mathbf{0} & \mathbf{0} \end{pmatrix} \mathcal{V}_{Q_L} \\ &= \bar{\mathcal{M}}_Q \Delta \mathcal{Z}_Q + \begin{pmatrix} \bar{M}_q & \mathbf{0} \\ \mathbf{0} & \mathbf{0} \end{pmatrix}. \end{aligned} \tag{A11}$$

On the other hand, by considering Eq. (6) for M_q and Δ'_{qQ} in $\mathcal{M}_Q$ we obtain Λ^H_Q in Eq. (26) as

$$\mathcal{V}^\dagger_{Q_R} \mathcal{M}_Q \begin{pmatrix} \mathbf{1} & \mathbf{0} \\ \mathbf{0} & \mathbf{0} \end{pmatrix} \mathcal{V}_{Q_L} = \frac{v}{\sqrt{2}} \mathcal{V}^\dagger_{Q_R} \begin{pmatrix} \lambda_q & \mathbf{0} \\ h_q & \mathbf{0} \end{pmatrix} \mathcal{V}_{Q_L}. \tag{A12}$$

Comparison of Eqs. (A11) and (A12) establishes the relation between the Z-boson coupling and the standard Higgs H coupling,

$$\Lambda^H_Q = (\bar{\mathcal{M}}_Q / v) \Delta \mathcal{Z}_Q + \begin{pmatrix} \bar{M}_q / v & \mathbf{0} \\ \mathbf{0} & \mathbf{0} \end{pmatrix}. \tag{A13}$$

Specifically, Eq. (31) is obtained from the upper diagonal block, and Eqs. (54) and (55) from the off-diagonal blocks with $\mathcal{Z}_Q[q^\dagger Q] = \Delta \mathcal{Z}_Q[q^\dagger Q]$.

Similarly, we obtain the relation between the Z-boson coupling and the singlet Higgs S_+ coupling as follows. By using Eq. (A10), we calculate

$$\begin{aligned} \mathcal{V}^\dagger_{Q_R} \mathcal{M}_Q \begin{pmatrix} \mathbf{0} & \mathbf{0} \\ \mathbf{0} & \mathbf{1} \end{pmatrix} \mathcal{V}_{Q_L} &= \bar{\mathcal{M}}_Q \mathcal{V}^\dagger_{Q_L} \begin{pmatrix} \mathbf{0} & \mathbf{0} \\ \mathbf{0} & \mathbf{1} \end{pmatrix} \mathcal{V}_{Q_L} \\ &= -\bar{\mathcal{M}}_Q \Delta \mathcal{Z}_Q + \begin{pmatrix} \mathbf{0} & \mathbf{0} \\ \mathbf{0} & \bar{M}_Q \end{pmatrix}. \end{aligned} \tag{A14}$$

On the other hand, by considering Eq. (7) for Δ_{qQ} and M_Q in $\mathcal{M}_Q$ we obtain $\Lambda^{S_+}_Q$ in Eq. (27) as

$$\mathcal{V}^\dagger_{Q_R} \mathcal{M}_Q \begin{pmatrix} \mathbf{0} & \mathbf{0} \\ \mathbf{0} & \mathbf{1} \end{pmatrix} \mathcal{V}_{Q_L} = \frac{v_S}{\sqrt{2}} \mathcal{V}^\dagger_{Q_R} \begin{pmatrix} \mathbf{0} & f^+_Q \\ \mathbf{0} & \lambda^+_Q \end{pmatrix} \mathcal{V}_{Q_L}. \tag{A15}$$

Comparison of Eqs. (A14) and (A15) leads to the expected relation

$$\Lambda^{S_+}_Q = -(\bar{\mathcal{M}}_Q / v_S) \Delta \mathcal{Z}_Q + \begin{pmatrix} \mathbf{0} & \mathbf{0} \\ \mathbf{0} & \bar{M}_Q / v_S \end{pmatrix}. \tag{A16}$$

Specifically, Eq. (32) is obtained from the upper diagonal block, and Eqs. (56) and (57) from the off-diagonal blocks with $\mathcal{Z}_Q[q^\dagger Q] = \Delta \mathcal{Z}_Q[q^\dagger Q]$.

[1] F. Gürsey, P. Ramond, and P. Sikivie, Phys. Lett. **60B**, 177 (1976); P. Langacker, Phys. Rep. **72**, 185 (1981); J. L. Hewett and T. G. Rizzo, Phys. Rep. **183**, 193 (1989).

[2] F. del Aguila and M. J. Bowick, Nucl. Phys. **B224**, 107 (1983); F. del Aguila and J. Cortés, Phys. Lett. **156B**, 243 (1985); F. del Aguila, M. K. Chase, and J. Cortés, Nucl. Phys. **B271**, 61 (1986).

[3] G. C. Branco and L. Lavoura, Nucl. Phys. **B278**, 738 (1986).

[4] V. Barger, R. J. N. Phillips, and K. Whisnant, Phys. Rev. Lett. **57**, 48 (1986).

[5] R. W. Robinett, Phys. Rev. D **33**, 1908 (1986).

[6] G. Eilam and T. G. Rizzo, Phys. Lett. B **188**, 91 (1987).

[7] P. Langacker and D. London, Phys. Rev. D **38**, 886 (1988).

[8] K. S. Babu and R. N. Mohapatra, Phys. Rev. Lett. **62**, 1079 (1989).

[9] L. Bento and G. C. Branco, Phys. Lett. B **245**, 599 (1990).

[10] Y. Nir and D. Silverman, Phys. Rev. D **42**, 1477 (1990); D. Silverman, Phys. Rev. D **58**, 095006 (1998).

[11] L. Lavoura and J. P. Silva, Phys. Rev. D **47**, 1117 (1993); **47**, 2046 (1993).

[12] G. C. Branco, T. Morozumi, P. A. Parada, and M. N. Rebelo, Phys. Rev. D **48**, 1167 (1993).

[13] G. C. Branco, P. A. Parada, and M. N. Rebelo, Phys. Rev. D **52**, 4217 (1995).

[14] V. Barger, M. S. Berger, and R. J. N. Phillips, Phys. Rev. D **52**, 1663 (1995).

[15] F. del Aguila, J. A. Aguilar-Saavedra, and G. C. Branco, Nucl. Phys. **B510**, 39 (1998).

[16] F. del Aguila, J. A. Aguilar-Saavedra, and R. Miquel, Phys. Rev. Lett. **82**, 1628 (1999); J. A. Aguilar-Saavedra and G. C. Branco, Phys. Lett. B **495**, 347 (2000); F. del Aguila, J. Santiago, and M. Pérez-Victoria, J. High Energy Phys. 09 (2000) 011.

[17] M. B. Popovic and E. H. Simmons, Phys. Rev. D **62**, 035002 (2000).

[18] P. H. Frampton, P. Q. Hung, and M. Sher, Phys. Rep. **330**, 263 (2000).

[19] Y. Takeda, I. Umemura, K. Yamamoto, and D. Yamazaki, Phys. Lett. B **386**, 167 (1996); I. Kakebe and K. Yamamoto, Phys. Lett. B **416**, 184 (1998).
[20] K. Higuchi and K. Yamamoto, Phys. Rev. D **62**, 073005 (2000).
[21] K. Higuchi, M. Senami, and K. Yamamoto, Phys. Lett. B **638**, 492 (2006).
[22] G. Barenboim, F. J. Botella, and O. Vives, Nucl. Phys. **B613**, 285 (2001); D. Hawkins and D. Silverman, Phys. Rev. D **66**, 016008 (2002); T. Yanir, J. High Energy Phys. 06 (2002) 044.
[23] J. A. Aguilar-Saavedra, Phys. Rev. D **67**, 035003 (2003); **69**, 099901(E) (2004).
[24] J. A. Aguilar-Saavedra, F. J. Botella, G. C. Branco, and M. Nebot, Nucl. Phys. **B706**, 204 (2005); F. J. Botella, G. C. Branco, and M. Nebot, Phys. Rev. D **79**, 096009 (2009).
[25] L. T. Handoko and T. Morozumi, Mod. Phys. Lett. A **10**, 309 (1995); **10**, 1733(E) (1995); C.-H. V. Chang, D. Chang, and W.-Y. Keung, Phys. Rev. D **61**, 053007 (2000); M. Aoki, E. Asakawa, M. Nagashima, N. Oshimo, and A. Sugamoto, Phys. Lett. B **487**, 321 (2000).
[26] A. K. Giri and R. Mohanta, Phys. Rev. D **68**, 014020 (2003); R. Mohanta and A. K. Giri, Phys. Rev. D **78**, 116002 (2008).
[27] C.-H. Chen, C.-Q. Geng, and L. Li, Phys. Lett. B **670**, 374 (2009).
[28] S. L. Glashow and S. Weinberg, Phys. Rev. D **15**, 1958 (1977); E. A. Paschos, Phys. Rev. D **15**, 1966 (1977).
[29] A. Antaramian, L. J. Hall, and A. Rašin, Phys. Rev. Lett. **69**, 1871 (1992); L. Hall and S. Weinberg, Phys. Rev. D **48**, R979 (1993).
[30] J. McDonald, Phys. Rev. D **53**, 645 (1996); T. Uesugi, A. Sugamoto, and A. Yamaguchi, Phys. Lett. B **392**, 389 (1997).
[31] G. C. Branco, D. Delépine, D. Emmanuel-Costa, R. González Felipe, Phys. Lett. B **442**, 229 (1998).
[32] F. del Aguila, G. L. Kane, and M. Quirós, Phys. Rev. Lett. **63**, 942 (1989); F. del Aguila, Ll. Ametller, G. L. Kane, and J. Vidal, Nucl. Phys. **B334**, 1 (1990).
[33] V. Barger and K. Whisnant, Phys. Rev. D **41**, 2120 (1990).
[34] T. C. Andre and J. L. Rosner, Phys. Rev. D **69**, 035009 (2004).
[35] J. A. Aguilar-Saavedra, Phys. Lett. B **625**, 234 (2005).
[36] Y. Grossman, Y. Nir, J. Thaler, T. Volansky, and J. Zupan, Phys. Rev. D **76**, 096006 (2007).
[37] S. Sultansoy and G. Unel, Phys. Lett. B **669**, 39 (2008).
[38] Z. G. Berexhiani, Phys. Lett. B **129**, 99 (1983); D. Chang and R. N. Mohapatra, Phys. Rev. Lett. **58**, 1600 (1987); A. Davidson and K. C. Wali, Phys. Rev. Lett. **59**, 393 (1987); **60**, 1813 (1988); S. Rajpoot, Phys. Lett. B **191**, 122 (1987).
[39] M. Bona *et al.* (UTfit Collaboration), J. High Energy Phys. 03 (2008) 049.
[40] G. Buchalla, G. Hiller, and G. Isidori, Phys. Rev. D **63**, 014015 (2000); C. Bobeth, G. Hiller, and G. Piranishvili, J. High Energy Phys. 07 (2008) 106.
[41] E. Barberio *et al.* (Heavy Flavor Averaging Group), arXiv:0808.1297.
[42] M. Misiak *et al.*, Phys. Rev. Lett. **98**, 022002 (2007).
[43] T. Becher and M. Neubert, Phys. Rev. Lett. **98**, 022003 (2007).
[44] V. Barger, P. Langacker, M. McCaskey, M. J. Ramsey-Musolf, and G. Shaughnessy, Phys. Rev. D **77**, 035005 (2008); **79**, 015018 (2009); V. Barger, H. E. Logan, and G. Shaughnessy, *ibid.* **79**, 115018 (2009).